DETERMINING THE VARIABILITY IN THE LUNG MICROBIOME THROUGHOUT THE COURSE OF MYCOBACTERIUM TUBERCULOSIS INFECTION

by

MacKenzie Marie Bryant

BS, Alfred State College - SUNY College of Technology, 2015

Submitted to the Graduate Faculty of

Infectious Diseases and Microbiology

Graduate School of Public Health in partial fulfillment

of the requirements for the degree of

Master of Science

University of Pittsburgh

2017

UNIVERSITY OF PITTSBURGH

Graduate School of Public Health

This thesis was presented

by

MacKenzie Marie Bryant

It was defended on

April 11th, 2017

and approved by

Thesis Advisor:
JoAnne L. Flynn, PhD, Professor, Department of Microbiology and Molecular Genetics, School of Medicine, University of Pittsburgh

Committee Member:
Joshua T. Mattila, PhD, Assistant Professor, Department of Infectious Diseases and Microbiology, Graduate School of Public Health, University of Pittsburgh

Committee Member:
Robbie B. Mailliard, PhD, Assistant Professor, Department of Infectious Diseases and Microbiology, Graduate School of Public Health, University of Pittsburgh

JoAnne L. Flynn, PhD

DETERMINING THE VARIABILITY IN THE LUNG MICROBIOME THROUGHOUT THE COURSE OF MYCOBACTERIUM TUBERCULOSIS INFECTION

MacKenzie Bryant, MS

University of Pittsburgh, 2017

ABSTRACT

Tuberculosis remains a major health threat throughout the world, despite having a vaccine and treatments. *Mycobacterium tuberculosis* (*Mtb*) infects alveolar macrophages in the lung and inflammation occurs after infection. The lung microbiome in regards to *Mtb* infection is poorly understood, and whether inflammation from infection affects the lung microbiome is unknown. The goal of our study is to determine whether *Mtb* induces a significant and durable change in the lung microbiome of cynomolgus macaques. We investigated and compared the community clusters between the lung and oral cavity, assessed how the diversity of the lung microbiota changes throughout infection, and associated these changes in the lung with inflammation. Bronchoalveolar lavage (BAL) was obtained pre-infection and at several time points post-*Mtb* infection, as well as oral wash and saline bronchoscope control samples from respective macaques. Operational taxonomic units (OTUs) were generated after 16s rRNA sequencing was performed once DNA was extracted from collected samples. We profiled microbial communities to see the community structure differences between oral and lung environment and show how the microbiome changes throughout infection. PET/CT imaging was used to visualize and quantify inflammation over the course of infection by using FDG avidity (total PET HOT). Our results show that the oral and lung compartments are distinct with regard to community

structure, distinct bacterial taxa are more relatively abundant in certain lobes, and lung inflammation and lung microbiome changes are variable within macaques and between macaques. Analysis of the first cohort of macaques (N=10) did not reveal correlations between lung inflammation and relative abundance or alpha-diversity, but our data is preliminary and based on small sample size. Our sample size will greatly increase after the second cohort of macaques are fully sequenced and analyzed. These changes and disruptions in the lung microbiome may have public health relevance in regards to overall lung health and may also play a role in the outcome of *Mtb* infection.

TABLE OF CONTENTS

LIST OF TABLES

LIST OF FIGURES

PREFACE

I would first like to thank Dr. JoAnne L. Flynn. Thank you for opening your doors to me and allowing me to become the first master's graduate student you've had in your lab. I have learned so much, and you have helped me fuel my passion of immunology. You have been a fantastic PI, and I thank you for your help, honesty, and ability to answer e-mails so incredibly fast!

I would like to thank the other members of my thesis committee – Dr. Joshua T. Mattila and Dr. Robbie B. Mailliard. Thank you so much for keeping me on track in regards to both my GSPH studies and my thesis project. You have both given me so many great ideas in order to further my success as a student and as a researcher.

Next, I would like to thank Dr. Anthony Cadena. You have been both my mentor and my friend during my time at Pitt. I've learned so much from you and am thankful to have been able to work with you.

Thank you to the entire rest of the Flynn lab. Every single one of you have helped me in some way, either by helping me out in the lab or by being a fantastic friend. I specifically want to thank Dr. Philana "Ling" Lin, Amy Fraser, Melanie O'Malley, and Tara Rutledge for their tremendous help with this project. Thank you, Pauline Maeillo, for your wizardly statistical knowledge and ability to make time for everyone no matter how busy you are.

Last but certainly not least, thank you to our collaborators at New York University: Dr. Elodie Ghedin, Tao Ding, Yixuan Ma, and Dayoon Kwon. You've all been fantastic to work with, and I'm so grateful for the knowledge I have gained from working with all of you.

1.0 INTRODUCTION

Tuberculosis remains a health treat throughout the entire world, despite having a vaccine and treatments. Development of nonhuman primate models that mimic many aspects of infection in humans helps researchers study the course of infection of *Mycobacterium tuberculosis (Mtb)*, as well as the pathogenesis, immune response, and host interactions during disease. Nonhuman primate models are also useful when studying the lung microbiome, an understudied field due to many obstacles regarding invalid beliefs of the lung, sample collection, and respiratory tract kinetics. The research in this thesis focuses on investigating the changes that the lung microbiome undergoes after *Mtb* infection. A longitudinal study of the lung microbiome and tuberculosis has never been performed before, and investigating how the lung microbiome changes after and throughout *Mtb* infection may give us insight about important aspects of infection and lung health.

1.1 TUBERCULOSIS

1.1.1 Epidemiology and Clinical Definitions

Tuberculosis (TB) remains a major health threat throughout the world. In 2015, there were 10.4 million new cases of TB, and 1.8 million people died from the disease[1]. TB mainly affects people

in low and middle-income countries. For example, the incidence of TB is >250-fold higher in South Africa than in the United States[2]. Of all worldwide TB cases, 60% occur in six countries: China, India, Indonesia, Nigeria, Pakistan, and South Africa[1]. Many areas that are affected by TB, such as Sub-Saharan Africa, are also afflicted by the HIV epidemic, resulting in even higher risk for development for active (symptomatic and transmissible) TB[3]. Although a vaccine and treatments exist for TB, vaccination yields partial protection (efficacies range from 0-80%)[4] and drug treatments are lengthy and intensive[3]. Lack of access to healthcare, rise of multi-drug resistant TB, HIV status, and other societal, environmental, and economical risk factors are also responsible for the high global burden of TB.

Robert Koch discovered the etiologic agent that causes TB, *Mycobacterium tuberculosis* (*Mtb*), in 1882[5]. *Mtb* infects via the lungs, but dissemination is possible. When an individual becomes infected with *Mtb*, 90-95% of people remain asymptomatic, which is termed latent TB infection (LTBI)[6]. The other 5-10% of people will develop active disease. Although one-third of the world's population is latently infected with *Mtb*, only 5-10% of these people will experience reactivation and develop active TB in their lifetimes[6]. In clinical terms, LTBI is asymptomatic and non-transmissible. In contrast to LTBI, active TB infection is transmissible via aerosolized droplets, and people with active disease experience a range of symptoms such as fever, fatigue, appetite loss, weight loss, and chronic cough[2]. Individuals who have LTBI or active disease will have a reaction to the tuberculin skin test (TST), which contains mycobacterial antigens, demonstrating an immune response to the bacteria. A non-infected person would not react to TST since their immune response has never seen these antigens before, therefore an immune response will not be elicited. During LTBI or active disease, IFN-gamma release assays (IGRA), which measure reactivity to *Mtb*-specific antigens, will also be positive[2].

1.1.2 The Spectrum of *M. Tuberculosis* Infection

It is now appreciated that strictly using 'latent' and 'active' to describe the disease status of an infected individual is not ideal. This is because disease status entails much diversity and can be described as a spectrum of disease, which can range from *Mtb* clearance to disseminated disease (Fig. 1)[2,7].

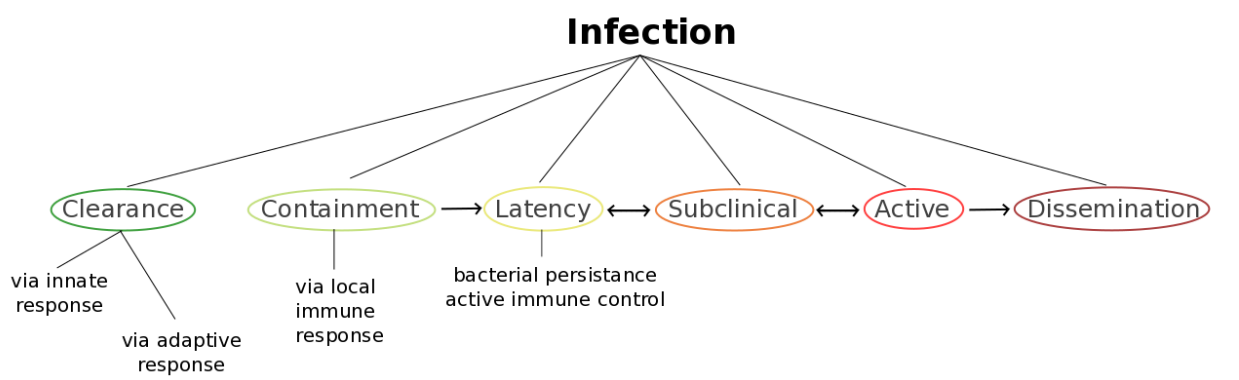

Figure 1. The spectrum of *Mtb* infection

After infection, many possible outcomes are possible. These can range from disease clearance (either via the innate immune response or the adaptive immune response) to complete *Mtb* systemic dissemination.

On the left-most side of the disease spectrum, one would have *Mtb* clearance via the innate immune response. These individuals do not develop an adaptive immune response to *Mtb*, resulting in negative TST and IGRA results. Bacterial clearance that is accompanied by the development of an adaptive immune response to *Mtb* is also possible; these individuals would have positive responses to immunological tests for TB[2]. In those who do not clear infection, the bacteria persist under strong host immune control ('true' LBTI)[7]. Further down the spectrum, there is subclinical infection. These individuals remain asymptomatic but are able to transmit *Mtb*, and may be culture positive, indicating active bacterial replication[8]. Patients who have active pulmonary (in the lungs) disease display symptoms, can transmit *Mtb*, and immune

responses and molecular diagnostic testing methods are all positive for bacterial presence. *Mtb* may disseminate, resulting in extra pulmonary TB or even miliary TB/sepsis[2,7].

1.1.3 Transmission and Immunology

Mtb infection is transmitted via inhalation of droplet nuclei that have been expelled from the lungs of an infected person with subclinical or active disease. The bacteria travel down into the lower respiratory tract where they reach the lungs. Once in the lungs, the bacteria are engulfed by alveolar macrophages via receptor-mediated phagocytosis[9]. Inflammation occurs post-infection, and the infected macrophages then invade the lung parenchyma leading to the recruitment of large amounts of immune cells[2,7].

The establishment of the adaptive immune response after *Mtb* infection occurs at a relatively slow rate. A positive tuberculin skin test, showing an adaptive immune response, occurs at roughly 6 weeks post-infection for humans and roughly 4-6 weeks post-infection in macaques[10]. The adaptive immune response in regards to TB infection is delayed due to a number of immunological hindrances in the process of antigen presentation, MHC class II loading, and T cell priming. As *Mtb* infects the alveolar macrophage, there may be defects in the innate inflammatory response and entry of antigen presenting cells, causing delays in APC loading, and T cell recruitment, ultimately delaying T cell priming in the mediastinal lymph nodes[11].

As *Mtb* continues to interact with alveolar macrophages and dendritic cells throughout infection, several pro-inflammatory cytokines (tumor necrosis factor-α, IL-12, and IL-23) are released, along with several chemokines such as CCL2, CCL5, and CXCL8[12]. IL-23 and IL-17 are also important players in T-cell dependent inflammatory responses during infection, as both

IL-17- and IL-23-deficient mice displayed a decrease in antigen-specific inflammatory responses[13,14]. Inflammatory events that occur after *Mtb* infection are regulated by IFN-y and IL-2 production by activated T cells that have been recruited to the infection site[15]. The pro-inflammatory response helps in granuloma formation and bacterial burden reduction, therefore it is crucial for infection control[12]. There are also a number of anti-inflammatory factors involved in the host response to TB such as Tregs, and the release of IL-10, IDO, and PD-1 that may be associated with both host control and bacterial persistence and evasion[16,17,18,19].

1.1.4 The Granuloma

As large amounts of immune cells are recruited due to chemokines released, a granuloma starts to form. The granuloma is the hallmark of TB. The granuloma is a highly organized structure composed of many different types of immune cells such as macrophages, monocytes, neutrophils, epithelioid cells, and multi-nucleated giant cells surrounded by an area of lymphocytes[20]. Figure 2 shows a cartoon diagram of the structure and organization of cell types located in a granuloma found in the lungs of an infected individual. Individual granulomas can differ in both structure and organization. The function of the granuloma has two main, yet contradictory, functions that both benefit the host and bacteria. The granuloma is the site of both host control of *Mtb* and *Mtb* persistence [21]. The accumulation of immune cells at the site of infection function to contain *Mtb* replication and prevent dissemination. However, *Mtb* can live and survive inside the granuloma by evading the host immune response.

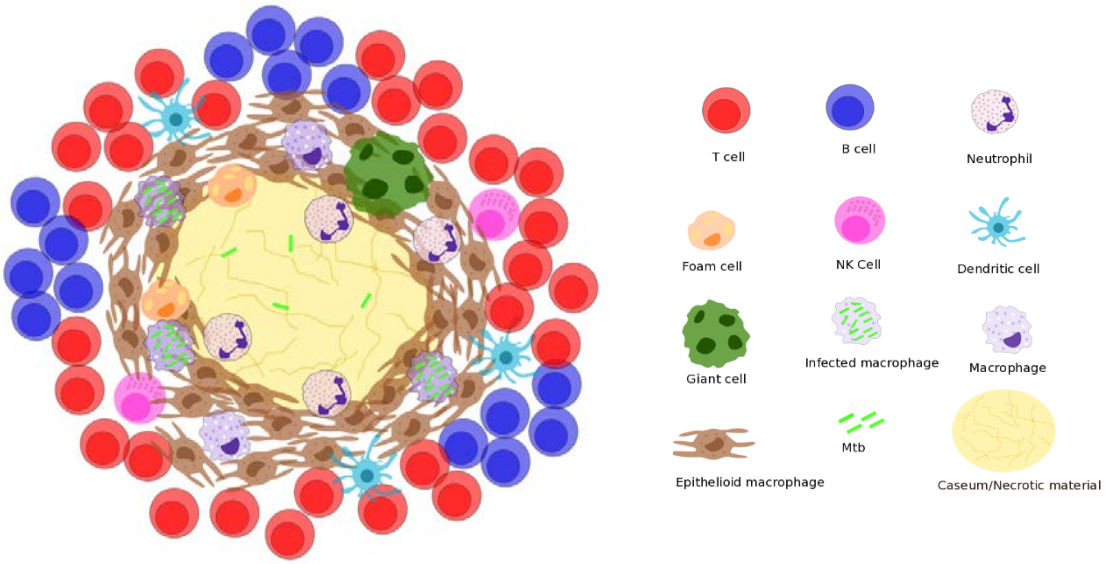

Figure 2. Structure and organization in a TB granuloma

A necrotic center is surrounded by a macrophage rich region, ultimately surrounded by a 'lymphocyte cuff' rich in T and B cells.

1.1.5 The Use of PET/CT Imaging to Track Granulomas

A valuable tool to track granulomas and inflammation over time is positron emission tomography (PET) fused with computed tomography (CT), using 2-deoxy-2-[^{18}F]-d-deoxyglucose (FDG) as a probe. FDG is taken up and retained by metabolically active cells, such as the cells of the TB granuloma. It has been shown that FDG avidity is increased when murine lymphocytes are activated by Con A[22], indicating that FDG uptake is increased during inflammation. Therefore, FDG avidity can be used as a general, nonspecific marker of inflammation. FDG avidity is normalized in order to give us a quantifiably measurable amount of inflammation within the granuloma, called total PET HOT.

PET/CT imaging has been extremely useful in studying TB infection and disease in macaques by allowing us to track granulomas and total inflammation over the course of infection. Coleman et. al (2014) has shown that by using early PET/CT scans, it is possible to

predict the outcome of TB disease[24]. Treatment efficacy can also be assessed using this method[25], simplifying processes that would otherwise be relatively more difficult to perform. By using serial PET/CT imaging techniques over the course of *Mtb* infection, granulomas and inflammation can be visualized over time. This imaging method, when used with the NHP model, allows us to study a wide range of questions regarding TB, such as inflammatory responses and infection dynamics, treatment efficacy, and disease outcomes.

Using [^{18}F] FDG PET/CT imaging, Lin et. al (2014) has shown that granulomas are both dynamic and independent, even within the same individual[23]. A granuloma in one area of a lung lobe of a macaque can slowly regress over time (Fig. 3) to the point where it may be difficult to even detect using PET/CT. In contrast, in another area of a lung lobe of the same macaque, granulomas can progress over time. Multiple granulomas can progress to such extremes that they can consolidate into one large granuloma.

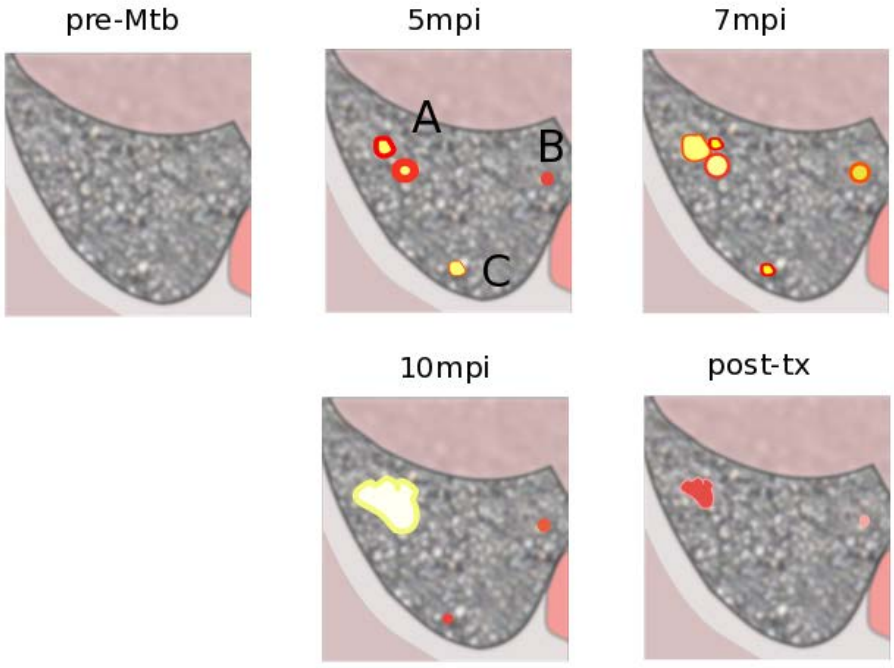

Figure 3. Hypothetical PET/CT image showing granuloma dynamism throughout time

In granuloma group A, granulomas progress through time and ultimately consolidate into one large granuloma. Granuloma B progresses until 7 months post-infection, but starts to regress by 10 months post-infection. Granuloma C regresses throughout infection. Regression occurs post-treatment; granuloma C cannot be detected on PET/CT post-treatment. (Information obtained from Lin, 2014[23]**)**

Granulomas also display a large range of structural heterogeneity, differing in cell composition and distribution. The necrotic granuloma is commonly found in active disease, and is composed of a non-cellular caseous center, epithelioid macrophage-rich middle region, ultimately surrounded by a well-defined 'lymphocyte cuff' of T and B cells[26]. Suppurative granulomas also have a well-defined lymphocyte cuff, an epithelioid macrophage-rich middle region, but contain centers that have high amounts of neutrophils. A fibrotic granuloma, commonly found in clinically latent TB, contains mineralized material surrounded by regions of fibrotic tissue[26]. Fibrotic granulomas usually have small numbers of lymphocytes and macrophages, and are considered a 'successful outcome'. When the host controls the *Mtb*, necrosis no longer occurs and the caseum is eventually replaced with this calcified and fibrotic material[27]. There are also non-necrotic granulomas, containing dense macrophage areas, random neutrophil distribution, and no caseous/necrotic material[26]. Ultimately, the unique dynamism and structural heterogeneity of each granuloma results in an immunological response that is quite variable from granuloma to granuloma and individual to individual.

Overall, TB displays a spectrum of outcomes over time. The infection is highly associated with a pro-inflammatory response, resulting in the hallmark of *Mtb* infection – the granuloma. Granulomas display large amounts of heterogeneity, and are independent and dynamic within individuals. The granuloma functions to immunologically contain the *Mtb*, and the *Mtb* can persist and survive within this structure. If a granuloma is unable to control infection, pathologies such as granuloma consolidation, cavity formation, TB pneumonia, or systemic spread may occur.

1.2 THE LUNG MICROBIOME

The microbiome can be defined as the microbiota, or microbes in a population, found in a specific place at a specific time[28]. Many studies have been performed investigating the effect of TB on the gut microbiome. One study has found that alteration of the gut microbiota results in immune control failure of TB infection –colonization with *H. hepaticus* resulted in a imbalance of *Mtb*-immune system crosstalk, resulting in lack of *Mtb* growth control, inflammation outbreaks, and increased lung pathology.[29] Another study found that altering the gut microbiota results in an increased susceptibility to TB[30], and it has been shown that *Mtb* infection results in a loss of diversity within the gut microbiota, possibly due to immune signaling between the lung and the gut[31]. However, regardless of TB being a respiratory disease, the lung microbiome with respect to *Mtb* infection remains poorly studied. This is due to many obstacles regarding defining the lung microbiome, sample collection, and general knowledge regarding the lung environment.

1.2.1 Obstacles in Studying the Lung Microbiome

One of the first obstacles that arose in the lung microbiome field was the long-standing belief that the normal lung was completely sterile. Although this claim was quite remarkable – a warm, moist mucosal environment that undergoes high airflow with the external environment, located just beneath the oropharynx, would be completely sterile – it was so embedded as common scientific knowledge that it was usually stated without question[32]. Many misunderstandings led to the origin of this belief. Culture-based methods that supplied poor growth conditions for

anaerobes were originally used to identify bacteria present in healthy lungs[33]. Absence of growth was misinterpreted as absence of bacteria in the lungs. This belief halted any preliminary lung microbiome research from occurring and was so firmly established that the Human Microbiome Project omitted the lung from its list of sampling sites from its first round of the project[34].

However, in the beginning of the 21st century, culture-independent methods such as 16S rRNA sequencing became more popular. Applications of culture-independent methods pertaining to the lungs were first used in patients with cystic fibrosis[35,36], showing a wide range of bacterial diversity in sputum samples. The use of bronchoalveolar lavage (BAL) samples allowed researchers to sample just the lower airways, showing that healthy airways did contain residential bacteria that were distinct from the upper airways, and the bacterial taxa found in healthy lungs were distinct from taxa found in diseased lungs[32]. These findings all invalidated the old belief that the healthy lung was sterile.

Although the statement of lung sterility was refuted, many obstacles remain regarding the lung microbiome. There remains a blurred line between the upper and lower respiratory tracts, which are diagramed in Figure 4. It is unknown how much the upper respiratory tract (URT) microbiome influences the lower respiratory tract (LRT) microbiome although many researchers have tried to address this question. One potential solution that has been attempted is to sample both the URT and LRT, and subtract the URT from the LRT[37]. However, a downfall to this methodology is that clinically important species that are in the LRT may also be present in the URT, and will get subtracted out and ruled as nonsignificant.

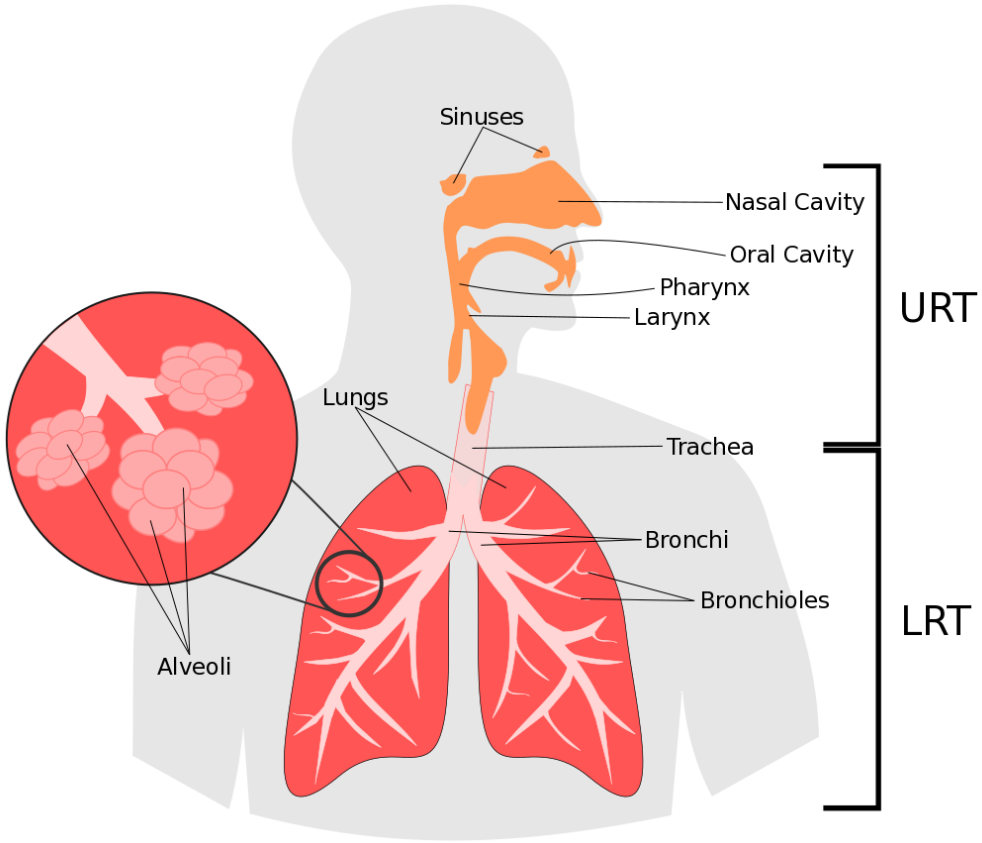

Figure 4. The respiratory tract

The respiratory tract of humans starts at the mouth/nose and then ends in the lungs. The upper respiratory tract consists of the nasal cavity, oral cavity, nasopharynx, oropharynx, laryngopharynx, larynx. The lower respiratory tract consists of the lungs, bronchi, alveoli. The trachea acts as the bridge between the upper and lower respiratory tracts and connects the larynx to the bronchial trees. (Information obtained from Huffnagle, 2016[38])

Another method that has been used is the application of the neutral theory of community ecology[39]. This theory states that all species in a community (the lung) are functionally equivalent, meaning species distribution is not due to environmental selection. Overall, the theory describes that microbes that differ significantly between sites (deviation from "neutrality") may be important species in the lung[40].

A second theory, the island model of biogeography, proposed by Dickson et. al, explains that the composition of the lung microbiome depends on immigration and elimination factors, as well as reproduction rates of the microbial community members[41]. Microbial immigration into

the lungs may occur due to microaspiration, bacterial inhalation via the air, or through direct mucosal dispersion. Elimination mechanisms may consist of cough, mucociliary clearance, and host immune defenses[41]. Examples of growth conditions that may affect microbial reproduction rates include changes in pH, temperature, nutrient availability, inflammatory cell concentration and/or activation, and oxygen tension[42]. However, none of these methods have become widely accepted in the field, leaving the overall question of how the URT and LRT influence each other, unanswered.

1.2.2 Contamination Controversies and Issues

An important difficulty that arises when performing research on the lung microbiome is the subject of sample collection. Ideally, one would want to obtain the lung tissue itself and digest the entire sample, allowing us to get the best representation of the lung microbiome without potential contamination of other microbes from other body sites[43] (Fig. 5). However, this is rarely feasible due to the highly invasiveness of collection procedures and cannot be used in longitudinal studies. For this reason, researchers tend to use either sputum or bronchoalveolar lavage (BAL) samples in order to simplify sample collection and accessibility. Sputum samples, although completely non-invasive allowing for longitudinal analysis, are always contaminated with microbes that are present in the oropharynx and other areas of the upper respiratory system[44]. Sputum sampling may also only sample higher sections of the lower respiratory tract. Sputum samples ultimately give a very inaccurate representation of the lung microbiome. Bronchoalveolar lavage (BAL) samples, obtained from a washing of the airways via bronchoscopy, are collected in a more invasive manner than sputum. However, unlike sputum, they give a better representation of the lung microbiome because the bronchoscope does not

collect from the upper respiratory tract, and mainly samples the lower respiratory tract[43]. Although a risk of potential contamination may still exist from the microbes that come into contact with the bronchoscope while it travels through the mouth and upper airways, BAL sampling is the 'happy medium' of lung microbiome sampling methods.

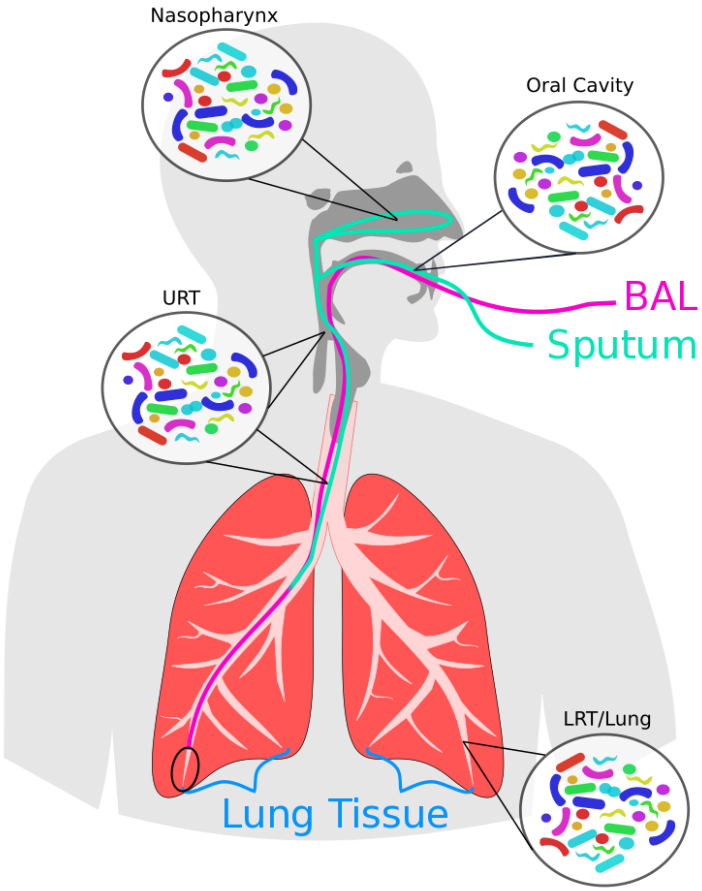

Figure 5. Potential sites for contamination while sampling the respiratory tract

Sputum samples may contain contamination from the URT, oral cavity, and nasopharynx. BAL samples may contain contamination from the URT if the bronchoscope has residual microbes from these sites. Ideally, one would sample the lung tissue itself, which samples only the LRT/lung microbiota with minimal contamination from other sites.

In addition to contamination due to sampling method, contamination may occur during sampling processing. Salter et. al has shown that bacterial DNA contamination is present in commonly used sterile laboratory reagents and also sterile reagents that are used in DNA

extraction kits[45]. The need for negative controls is absolutely crucial because the lung contains such a small level of bacteria that any sort of contamination may be significant. Negative controls can consist of kit reagent controls, PBS extraction controls, and a bronchoscope wash control in order to control for every step of the sample collection and extraction processes.

1.2.3 Lung Disease, Dysbiosis, and Inflammation

Past studies have shown that the lung microbiome is important in respiratory diseases such as asthma[32,46], COPD[47,48], cystic fibrosis[49], and pneumonia[41]. According to the island model of biogeography proposed by Dickson et al., in a state of lung disease, immigration and elimination becomes unbalanced and growth conditions are altered[41]. Microbial immigration may be increased due to gastroesophageal dysfunction[50]. Elimination may be increased due to cough or host inflammatory cell activation. As lung disease progresses, the lung environment shifts, changing growth conditions and ultimately altering the reproduction rates of lung microbiota. For example, inflammation of the respiratory tract during cystic fibrosis increases mucus production, resulting in low-oxygen pockets and increased temperature of the environment of the lung[51,52]. This change in environment may favor the growth of certain bacterial species. Overall, lung disease causes changes in immigration and elimination factors as well as changes in growth conditions, ultimately changing the composition of the lung microbiome. The microbial imbalances caused by lung disease can be described as dysbiosis.

Microbial dysbiosis that occurs from lung disease not only is caused by inflammation, but can also cause inflammation. This results in a positive feedback dysbiosis-inflammation loop[41], shown in Figure 7. This model states that when an inflammatory event occurs, such as an infection or allergy trigger, the host inflammatory response alters the lung microenvironment,

which in turn changes the growth conditions, resulting in dysbiosis of the microbiome composition. Some microbial species are favored to grow, and some species cannot continue to grow – this changes the microbiome. New species or species that newly become dominant in the lung results in a disruption in the homeostasis of the airway microbiome, causing *respiratory* dysbiosis. This respiratory imbalance in turn causes even more inflammation due to the detection of PAMPs on new or newly dominant microbial species. This inflammation further changes the growth conditions of the lung, creating a positive feedback loop.

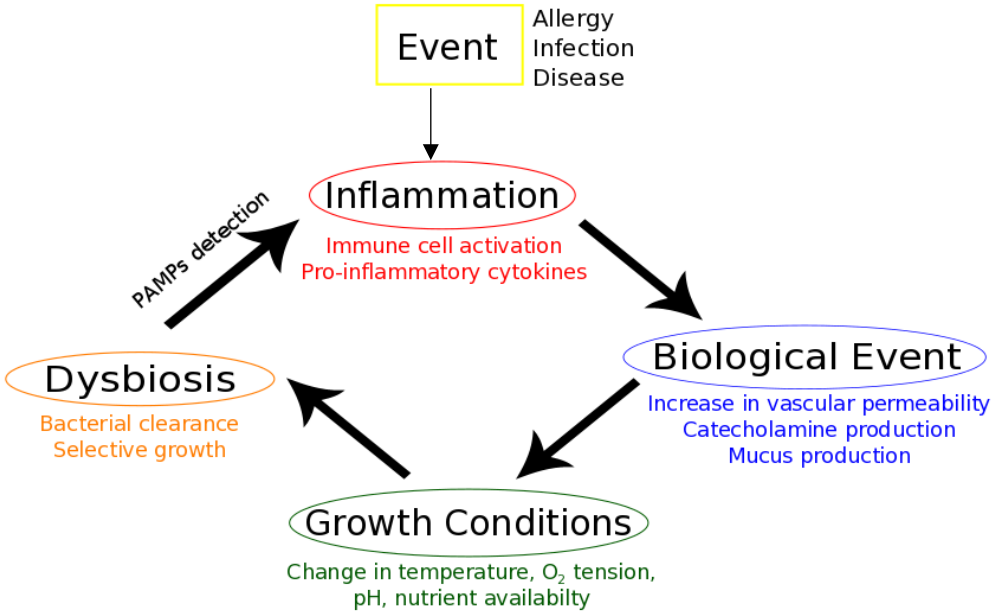

Figure 6. The inflammation-dysbiosis cycle

An inflammatory event occurs, causing many events in the body to occur such as mucus production, catecholamine production[53], and an increase of vascular permeability and free ATP[54], changing growth conditions such as temperature, oxygen tension, pH, and nutrient availability. A change in growth conditions creates dysbiosis by bacterial clearance and selective growth for certain species of bacteria. More inflammation results from this dysbiosis through the immune responses initiated from PAMPs detection of the new bacterial species, causing a positive-feedback dysbiosis-inflammation loop. (Information obtained from Dickson, 2014[41])

Overall, the lung microbiome remains largely unstudied due to the blurred line between the URT and LRT and potential contamination issues. Many researchers are finding ways to overcome these obstacles, but not one method has been widely accepted. Inflammation from

infection or another inflammatory event changes elimination and immigration factors and alters growth conditions of the lung, ultimately creating dysbiosis. This dysbiosis creates an imbalance in the homeostatic environment of the lung, thereby creating more inflammation. This inflammation further alters growth conditions, further changing the lung microbiome, causing a positive feedback loop of inflammation and dysbiosis.

1.2.4 The Lung Microbiome and *M. tuberculosis* Infection

Few studies have been performed investigating TB and the lung microbiome, and results have been inconsistent. One of the first TB microbiome studies in 2012 concluded that both healthy and *Mtb*-infected lungs were dominated by *Firmicutes* and *Bacteroidetes* and also shared *Proteobacteria, Actinobacteria*[28]. A second study investigating the differences between *Mtb*-infected and healthy lungs found *Proteobactera* and *Bacteroidetes* were the dominating microbiota in *Mtb*-infected lungs, while *Firmicutes* dominated in healthy control lungs[55]. Botero et al. (2014) concluded that *Bacteroidetes, Fusobacteria,* and *Actinobacteria* were the dominating microbiota in *Mtb*-infected lungs[56]. A fourth study found *Streptococcus, Gramulicatella,* and *Pseudomonas* dominating in *Mtb*-infected lungs, while healthy lungs had dominant populations of *Treponema, Catonella,* and *Coprococcus*[57]. Lastly, a study performed in 2016 found that the relative abundance of *Firmicutes* and *Actinobacteria* was significantly higher in TB samples compared healthy controls, where *Bacteroides* and *Proteobacteria* were found to be higher[58]. The findings of these studies are summarized in Table 1, which highlight the variability between the results of the studies. These studies used sputum samples, which is not ideally representative of the lower lung microbiome due to high amounts of contamination from the mouth and upper airways. These studies also had relatively small sample sizes, making it

harder to find consistencies and trends. Lastly, these studies were cross-sectional, not allowing the researchers to assess the changes of the microbiome over time within the same individual. Cross-sectional studies make it difficult to investigate how infection impacts the microbiome because the microbiome is so variable between individuals. Since the microbiome varies across individuals, cross-sectional studies make it difficult to determine changes induced by infection, as this would require extremely large sample sizes.

A recent study using human BAL samples as their sampling method found *Cupriavidus* to be the dominating genus in *Mtb*-infected lungs, while *Streptococcus* was the dominating genus found in healthy lungs[59]. It was mentioned that the generally low quantities of colonizing bacteria found in the lung made it difficult to obtain ideal PCR-amplified production of microbial DNA. Taken together, the past studies that investigate TB and the lung microbiome are limited and inconsistent; this is due to past misinformation about the lung being sterile (causing many people to disregard studying the lung microbiome), small sample size, and non-ideal sampling methods.

Table 1. Previous lung microbiome and TB studies

Study	Taxa highest in Healthy Lungs	Taxa highest in TB Lungs	Sampling Method
Cui, 2012[28]	*Firmicutes* *Bacteroidetes* *Proteobacteria* *Actinobacteria*	*Firmicutes* *Bacteroidetes* *Proteobacteria* *Actinobacteria*	Sputum
Cheung, 2013[55]	*Firmicutes*	*Proteobactera* *Bacteroidetes*	Sputum
Botero, 2014[56]		*Bacteroidetes* *Fusobacteria* *Actinobacteria*	Sputum
Wu, 2013[57]	*Treponema* *Catonella* *Coprococcus*	*Streptococcus* *Gramulicatella* *Pseudomonas*	Sputum
Krishna, 2016[58]	*Bacteroides* *Proteobacteria*	*Firmicutes* *Actinobacteria*	Sputum
Zhou, 2015[59]	*Streptococcus*	*Cupriavidus*	BAL

Overall, the lung microbiome in *Mtb* infection is largely unstudied. Conclusions obtained from past research have been inconsistent. Most past studies were also not ideal in regards to sampling method, sample collection timing (cross-sectional vs. longitudinal) and consisted of small sample sizes.

1.3 THE MACAQUE MODEL AND ITS IMPORTANCE IN TUBERCULOSIS AND MICROBIOME STUDIES

1.3.1 The NHP Model and Tuberculosis

Nonhuman primates (NHPs) are an incredibly valuable model to use in research. NHPs are closest to humans genetically compared to other animal models such as mice, Guinea pigs, rabbits or zebrafish, resulting in many similarities in immunology, pathogenesis, and host/pathogen interactions between NHPs and humans. The macaque model is an ideal animal model for both TB studies and microbiome studies.

Rhesus macaques (*Macaca mulatta*) and cynomolgus macaques (*Macaca fascicularis*) are two macaque species primarily used in TB studies. Macaques display several similarities to humans in regards to *Mtb* infection; immunology, disease outcome, clinical presentation, pathology, and pathogenesis in macaques species are comparable to TB in humans[60].

Previously used scientific animal models, such as the mouse model, are practical and relatively inexpensive but aren't ideal to study the pathogenesis and pathology of *Mtb* infections. In mice, TB granulomas are poorly organized and lack necrosis, unlike in human TB. It is also important to note that mice do not display any sort of latent infection; bacterial counts remain

high throughout the infection, which progresses until the mouse ultimately dies[61]. In contrast, macaques display a large range of pathology throughout the course of *Mtb* infection that represents the entire clinical spectrum of TB that is seen in humans[62]. Rhesus macaques, when infected with low-dose virulent *Mtb*, almost always develop active TB. In contrast, when cynomolgus macaques are infected, an equal proportion of monkeys will develop active disease and latent infection (LTBI)[62]. The use of the cynomolgus macaque model is a fantastic tool that allows researchers to study the entire disease spectrum of *Mtb* infection, representing human disease.

One of the most important comparisons between the macaque model and humans is the similarities in TB granulomas. Granulomas in macaques have a large range of variable granuloma heterogeneity. Caseous, suppurative, and non-necrotizing granulomas have been found, and some of these granulomas have been mineralized or largely fibrocalicified[63]. The similarities seen in granuloma heterogeneity, organization, and variability between macaque and human granulomas allows us to study granulomas and local immune responses more in depth.

1.3.2 The NHP Model and the Lung Microbiome

The use of the NHP model in microbiome studies is an excellent opportunity to increase our understanding of the lung microbiome composition and how it changes through time. Using a research model allows us to collect serial samples throughout the course of *Mtb* infection, allowing us to study the microbiome shifts over time. In humans, it is harder to obtain serial sampling of BAL because of the relative invasiveness of the procedure. The use of a NHP model also allows us to assess pre- and post-infection changes in the lung microbiome, potentially indicating certain bacterial taxa that are important in the course of infection or disease

progression. Variables that may alter results, such as diet or environmental conditions, can be controlled in an experimental setting unlike in humans that are sampled from the population. Inoculum dose and time of infection are also well-controlled. Importantly, the NHP model is useful as a bridge to human studies because it has been shown that the composition of the NHP gut microbiome is more similar to humans than other animal models[64]. Like humans, NHPs are also outbred[65], creating a diverse population variability that is similar to human variability. The use of macaques as an *in vivo* model is ideal for studying the changes of the lung microbiome in regards to *Mtb* infection.

2.0 STATEMENT OF INTENT, HYPOTHESIS, AND SPECIFIC AIMS

A longitudinal study investigating the changes of the lung microbiome before, during, and after *Mtb* infection has not been reported. For our study, the main goal was to assess whether *Mtb* infection induces a significant change in the lung microbiome in macaques. We hypothesized that inflammation from *Mtb* infection influences the variability of the lung microbiome in macaques. These changes and disruptions in the lung microbiome may have implications for overall lung health and also may play a role in the outcome of *Mtb* infection. We first determined the identity and compared community clusters of the lung and oral cavity in macaques to investigate how the oral cavity influences the lung. Second, we investigated the community structure and stability of the lung microbiome throughout the course of *Mtb* infection in macaques, allowing us to see how the lung microbiome changes throughout the course of infection. Lastly, we investigated whether the microbiota variability in the lung was associated with inflammation. BAL samples collected from macaques at different time points before and after infection were sequenced. The composition, diversity, and variability of the lung microbiome throughout the course of infection was determined. With this information, we investigated whether variability of the lung microbiome correlated with the variability of inflammation throughout infection, indicating that the inflammation due to *Mtb* infection changes the lung microbiome in macaques. This project is a collaboration with the Ghedin Lab (NYU), who performed the 16S sequencing and some statistical analyses.

2.1 SPECIFIC AIM 1: IDENTIFY AND COMPARE COMMUNITY CLUSTERS OF THE LUNG AND ORAL CAVITY IN MACAQUES.

One of the main questions in lung microbiome studies is how much the microbiota of the oral cavity (the URT) influences that of the lung. Using a cynomolgus macaque model, we obtained both oral and BAL samples to be sequenced to identify the composition of each respective environment. 16S rRNA sequencing helped generate OTUs which made comparing the relative abundance and composition of the oral cavity and lung microbiota. Alpha-diversity was determined between the two sampling sites, and a principle coordinate analysis was performed to further distinguish the differences between the oral and lung spaces. This aim will provide crucial data of the similarities and differences between the oral cavity (and URT) and the LRT. We hypothesized that there will be a difference in community structure between the oral cavity and lung.

2.2 SPECIFIC AIM 2: INVESTIGATE THE COMMUNITY STRUCTURE AND STABILITY OF THE LUNG MICROBIOME THROUGHOUT THE COURSE OF *M. TUBERCULOSIS* INFECTION IN MACAQUES.

How the lung microbiome changes throughout the course of *Mtb* remains largely unstudied. BAL samples were obtained from time points from before and after *Mtb* infection to study the changes throughout infection. Obtaining samples before infection and 1, 4, and 5 months post-infection made it possible to study the changes in the OTU composition and relative abundance change in

the microbiota present in the lung throughout infection. We hypothesize that there will be a change in the overall stability and composition of the lung microbiome after *Mtb* infection.

2.3 SPECIFIC AIM 3: ASSOCIATE MICROBIOTA VARIABILITY IN THE LUNG WITH INFLAMMATION.

Inflammation plays a large role in *Mtb* infection and is important in the immunology of the granuloma. We evaluated how levels of inflammation vary over time in individual macaques using PET/CT imaging. By quantifying overall FDG avidity, we have a measure of total inflammation, referred to as 'total PET HOT'. We then investigated whether there is an association between the variability of the lung microbiome and the changes of inflammation throughout *Mtb* infection by assessing the correlations between total PET HOT, relative abundance, and alpha-diversity over time. If there is a correlation between microbiome variability and PET HOT, we will investigate if inflammation caused by infection creates these changes in the composition of the lung microbiome.

3.0 METHODS

3.1 INFECTION AND NHP MODEL

Twenty-six cynomolgus macaques (*Macaca fascicularis*) were used for this study. Macaques were obtained from Valley Biosystems (Sacramento, CA) and housed in designated biosafety level 3 (BSL-3) laboratory animal space at the University of Pittsburgh. All macaques receive essentially the same diet, including enrichment foods, and are housed in the same facility. Monkeys used for this study were parts of separately funded studies. We often perform serial BALs as a normal procedure throughout infection. The BAL collection procedure for the microbiome studies were performed slightly different than usual BAL collection procedures, explained below. These monkeys remain un-manipulated other than *Mtb* infection during the period of microbiome sampling.

Macaques were infected with <25 CFU *Mtb* strain Erdman via bronchoscopic instillation into the lower lung, as previously described in [66] and [67]. PET/CT imaging was used post-infection to determine which lobe was successfully infected, as well as subsequent lobe involvement due to dissemination of the infection.

3.2 BRONCHOALVEOLAR LAVAGE COLLECTION

Oral, saline/bronchoscope control wash, and right and left lower lobe samples were collected approximately 3 weeks pre-infection and approximately 1, 4, and 5 months post-infection. Oral

washes were obtained by a 5mL rinse of a cheek pouch. Bronchoscope washes were obtained by a 5mL saline wash of the sterilized instrument. The monkeys' mouths were swabbed with antiseptic chlorohexane immediately prior to the insertion of the bronchoscope for BAL collection, minimizing contamination from the oral cavity. A 7mL lavage of the left lower lobe is performed, followed by sterilization of the bronchoscope via antiseptic solution (Cidvex, Civco Medical Solutions) and lavage of the right lower lobe is performed thereafter. Lavages yield approximately 4-5 mL from each lobe. After collection lavages were immediately aliquoted into 4.5 mL cryovials and frozen at -80°C until time of DNA extraction. Overall, each macaque will have 4 samples at each time point (oral wash, saline bronchoscope wash, right lower lung, and left lower lung), ultimately yielding 372 total samples. For this study, data from the first 10 monkeys were analyzed. An additional data set from 16 more monkeys is awaiting sequencing and analysis.

3.3 DNA EXTRACTION/ISOLATION

DNA extraction was performed on all collected samples. Previously collected samples were removed from -80°C, thawed, and centrifuged. The PowerSoil® DNA Isolation Kit (MO BIO) was used in which BAL samples (containing liquid and cells) were thoroughly homogenized and lysed, then bound to a silica membrane in order to capture DNA for DNA elution. This kit incorporated the use of bead-beating tubes to ensure thorough homogenization and cell lysis.

Extraction was performed in BSL-3 laboratory conditions under a biological safety cabinet using sterile technique. Reagent controls and PBS controls were performed for each monkey to assess any residual DNA from kit reagents, tubes, and pipette tips. Proper PPE was

worn at all times, and BSL-3 protocols were followed. Measures were taken to minimize contamination, such as using ultra-violet light and bleach to sterilize the working space and equipment before extraction, changing gloves after every centrifugation step, only extracting DNA from one macaque at a time to minimize cross-contamination between monkeys, using a microcentrifuge specific to DNA extractions that is kept under a biosafety cabinet at all times, and using designated pipettes and sterile tips.

3.4 16S RRNA SEQUENCING AND DATA ANALYSIS

Sample preparation for 16S rRNA sequencing and sequencing of DNA eluted from BAL samples was performed by Dr. Elodie Ghedin and lab members (NYU). Barcodes were added to DNA to prime the target V4 hypervariable amplicon. Amplicons were purified and library preparation was performed using the KAPA HTP Library Preparation Kit (KAPA Biosystems). Primer dimers were removed and confirmation of removal was given by TapeStation (Agilent Genomics). Library quantification was performed using the KAPA Library Quantification Kit (KAPA Biosystems), which contain DNA standards, 10X Primer Premix, and KARA SYBR® FAST qPCR Kits, to quantify the number of amplifiable molecules in the prepared Illumina library.

After qPCR was performed, the V4 region was sequenced using the MiSeq (Illumina) instrument. The Mothur pipeline, modified for the MiSeq platform, includes the removal of low quality reads, chimeras (UCHIME), non-mate-paired reads, and merging of paired-end reads. Classification of sequences to the genus level was made by using the RDP (Ribosomal Database Project) classifier. Operational Taxonomic Units (OTUs) were generated by clustering sequences

that share ≥97% nucleotide identity similarities (UCLUST). The 'top 10 OTUs' were generated by choosing the OTUs that had the highest proportion of reads present in the BAL samples. Using the taxonomic assignments and OTU-based profiles generated from sequencing data, many ordination, clustering, and community structure analyses were performed. Abundance and ubiquity between samples were visualized using CORBATA and QIIME.

3.5 PET/CT IMAGING

PET/CT scans were obtained from macaques at different time points post-infection, as described in [24] and [25]. ^{18}F-fluorodeoxyglucose (FDG) was used as a probe to label metabolically active cells, serving as a nonspecific marker of inflammation. FDG avidity can give us total PET HOT, allowing us to obtain a quantifiable measure of inflammation over time. FDG avidity is normalized to each macaque's dorsal muscle, individually, allowing us to normalize baseline inflammation.

3.6 STATISTICAL ANALYSIS

Statistical analysis in regards to the lung microbiome portion of the study was performed by Dr. Elodie Ghedin and lab members (NYU). Analyses were performed on an integrated QIIME and R package. Whole community structure changes were analyzed via Adonis. PCoA plot was generated by Yixuan Ma, Ghedin Lab, and used with permission.

Statistical analyses were performed at the University of Pittsburgh using JMP Pro 11 and Graphpad Prism 6, with the help of Pauline Maiello. Wilcoxon rank sum analyses were performed to determine differences of individual OTUs between involved and uninvolved lobes, differences over time, and differences between the oral cavity and lower lobe samples. Individual OTU relative abundance correlations (at four months post-infection) were performed using a Spearman's **ρ** Correlation, as were correlations between the ranges of OTU relative abundances and range of total PET HOT. Spearman's **ρ** and Pearson's r were used for analyzing the correlation between alpha-diversity and total PET HOT over time and range of diversity and range of total PET HOT of involved lobes, respectively. An unpaired t-test was performed to compare the range of diversity over time between involved and uninvolved lobes. Diversity was determined by the Inverse Simpson Index. Multiple-lobe involvement was accounted for in analyses.

4.0 RESULTS

4.1 EXPERIMENTAL OVERVIEW

To investigate the changes in microbiome variability throughout the course of *Mtb* infection, samples were collected at multiple time points (Fig. 7, top) from macaques. Oral cavity swab samples were collected to assess differences in microbial diversity (species richness and evenness) between the oral cavity and lung samples. A bronchoscope saline wash was performed to control for any residual DNA on the bronchoscope during sample collections (Fig. 7, bottom). PET/CT imaging was also performed 1, 4, and 5 months post-infection.

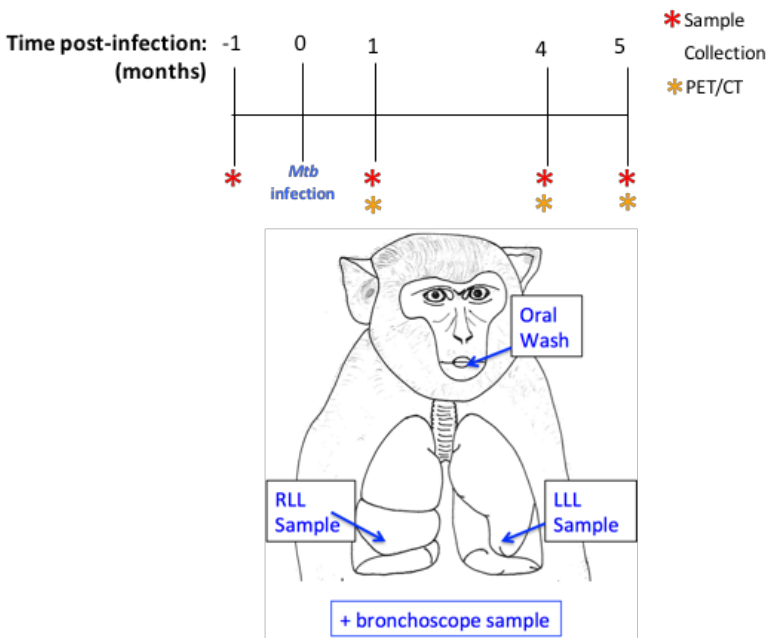

Figure 7. Experimental layout of sample collection sites and timeline

Oral wash, right lower lobe (RLL), left lower lobe (LLL), and saline bronchoscope wash samples were collected before *Mtb* infection and 1, 4, and 5 months post-*Mtb* infection.

Two cohorts of 10 and 16 macaques were used in this study yielding a total of 424 samples, including reagent and PBS controls during DNA extraction (Table 2).

Table 2. Sample distribution of cohorts

Cohort	# of Macaques	# BAL Samples	# Oral Wash Samples	# Bronchoscope Controls	# Reagent Controls	Total
1	10	70	36	36	20	162
2	16	114	58	58	32	262

4.2 THE ORAL CAVITY AND LUNG COMMUNITY STRUCTURES ARE DISTINCT

To determine how the community structures between the oral cavity and the lung differ, 16S rRNA sequencing was performed on oral cavity swab samples and bronchoalveolar lavage (BAL) samples. Sequencing was performed by the Ghedin Lab, NYU and the resulting data was used with permission. Lobe involvement is determined by inflammation: lobes that displayed inflammation via PET/CT imaging were grouped as ‘involved lobes’, and lobes that displayed no inflammation via PET/CT imaging were grouped as ‘uninvolved lobes’. It is important to note that absence of inflammation does not necessarily mean absence of infection; it is possible to have granulomas that are not FDG avid in a lobe, and therefore minimal inflammation. The following presented data are for the first cohort of N=10 macaques. The second cohort of N=16 macaques are being sequenced and analyzed. Thus, the following data is preliminary.

The genetic diversity between oral and lung BAL samples was visualized through the use of a principle coordinate analysis (Fig. 8). The data shows that oral samples cluster tightly together in one space, away from BAL samples, while the BAL samples cluster together in a different space. There is no pronounced difference in clustering between involved and uninvolved lobes. This data suggests that the genetic diversity of the oral cavity microbiome and the lung microbiome are distinct from one another, suggesting that the lung microbiome is not strictly just contamination by the oral cavity when the BAL washes were performed.

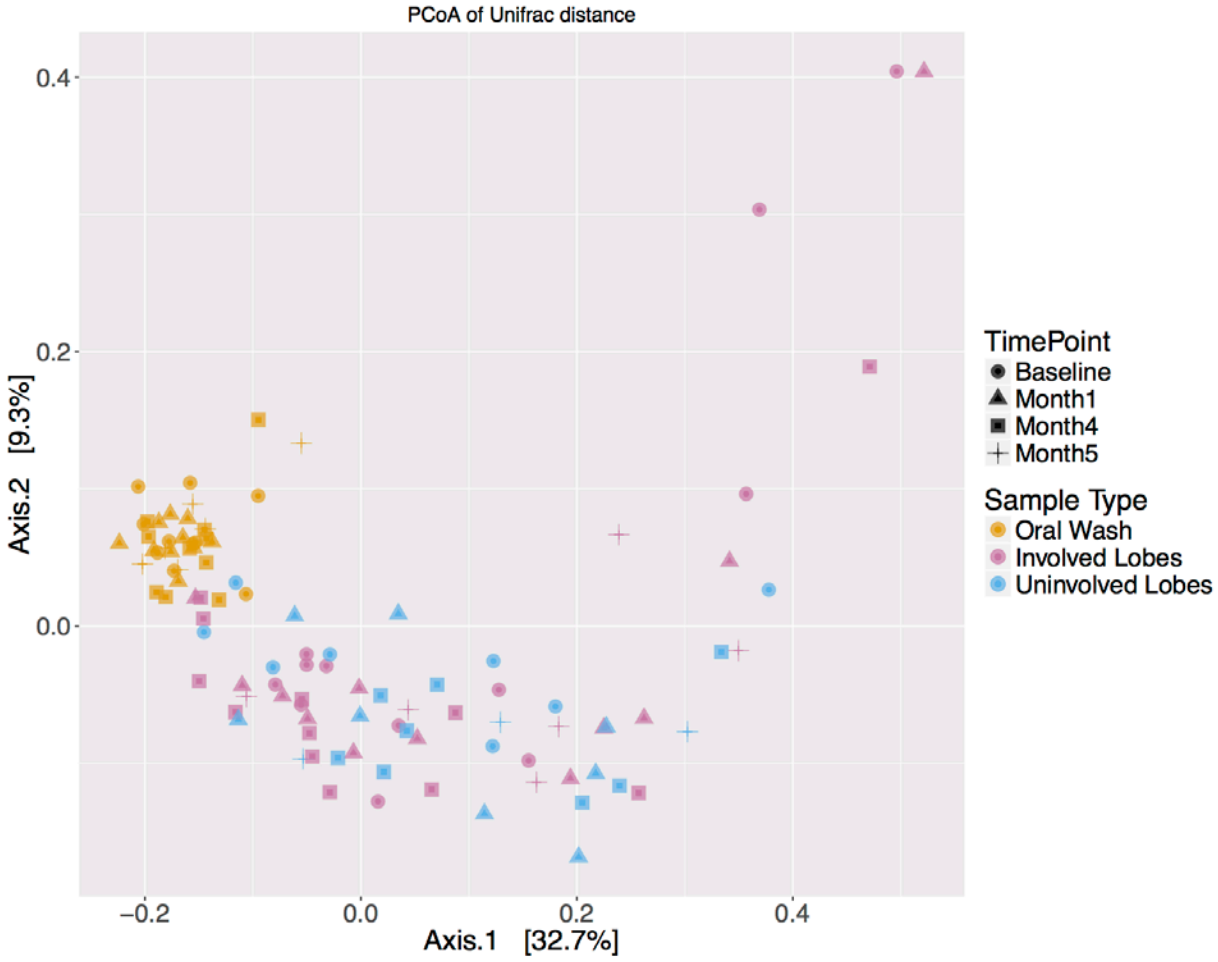

Figure 8. Principle coordinate analysis comparing the genetic diversity between oral wash and lung BAL samples

Oral wash samples (orange) cluster together, while lung BAL samples (pink and blue) cluster together in a different space. Graph generated by Yixuan Ma, Ghedin Lab, and used with permission.

Operational taxonomic units (OTUs) were generated by UCLUST, clustering together sequences that shared ≥97% nucleotide identity similarities. Our 'top 10 OTUs' were generated: *Burkholderia* (genus-level), *Actinomycetales* (order-level), *Actinobacillus* (genus-level), *Neisseria* (genus-level), *Aggregatibacter* (genus-level), *Moraxellaceae* (family-level), *Fusobacterium* (genus-level), *Acinetobacter* (genus-level), *Gemellaceae* (family-level), and *Streptococcus* (genus-level). These OTUs had the highest proportion of reads present in the BAL and oral wash samples after sequencing (data not shown). To assess whether there was a compositional difference between the oral wash samples and lobe samples in regards to the top 10 OTUs, the relative abundances of the top 10 OTUs were determined for the oral wash, involved lobe, and uninvolved lobe samples (Fig. 9). Relative abundance is relative to all OTUs found in the sample. Four of the top 10 OTUs were found in noticeably higher proportions in lobe samples vs. oral samples (*Burkholderia*, *Actinomycetales*, *Moraxellaceae*, and *Acinetobacter*), showing that a compositional difference between oral wash samples and lower lobe does exist. This further confirms our observation that the lung microbiome has a distinct composition than the oral cavity microbiome.

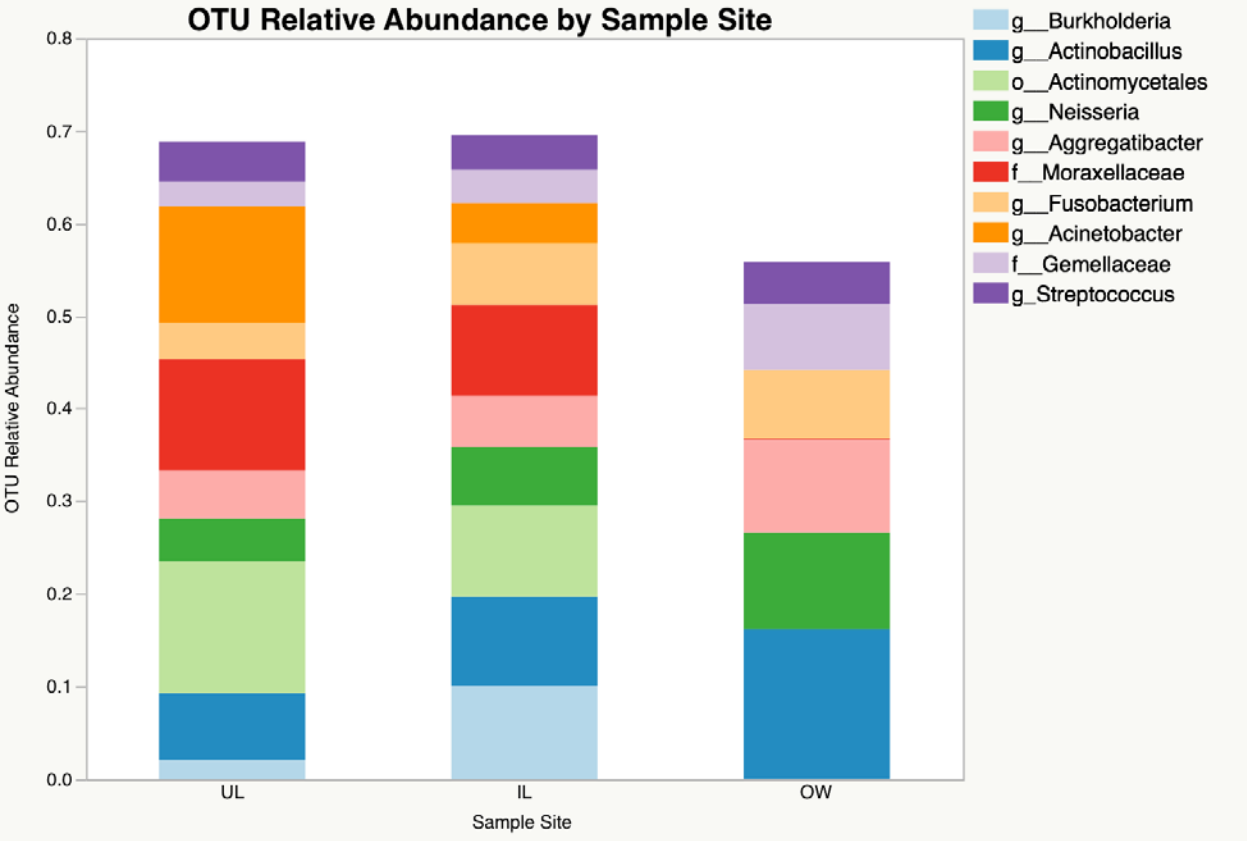

Figure 9. Relative abundance of top 10 generated OTUs between oral wash, involved lobe, and uninvolved lobe samples

Relative abundance is relative to all OTUs found in the sample.

To determine how lung and oral microbiome species diversity changes over time, the community alpha-diversity was determined by using the average Inverse Simpson Index for saline bronchoscope wash, oral wash, involved lobe, and uninvolved lobe samples at each time point (Fig. 10). A high Inverse Simpson Index confers a higher level of alpha-diversity. Oral wash, involved lobes, and uninvolved lobes were compared to one another to determine any trends of alpha-diversity. Our results show that the oral microbiome maintains a high amount of alpha-diversity pre-*Mtb* infection and throughout the entire course of infection. The oral wash

had a significantly higher level of alpha-diversity compared to all lung samples (p=0.0001, Wilcoxon rank sums).

The stable, high level of alpha-diversity of the oral cavity contrasts with the lobe samples, which have more variability in alpha-diversity over time. Alpha-diversity is variable in lobe samples throughout the course of *Mtb* infection, increasing and decreasing at different time points. There is a trend towards more species diversity in the involved vs. the uninvolved lobes 4 months post-infection (p=0.0574, Wilcoxon rank sums). Our results also show that the saline bronchoscope control wash maintains a low level of alpha-diversity before and throughout infection, implying that there is minimal contamination from the upper respiratory tract when collecting BAL samples. It is important to reiterate that these data represent only the first cohort of macaques (N=10), so the trend may become more pronounced as the sample size increases.

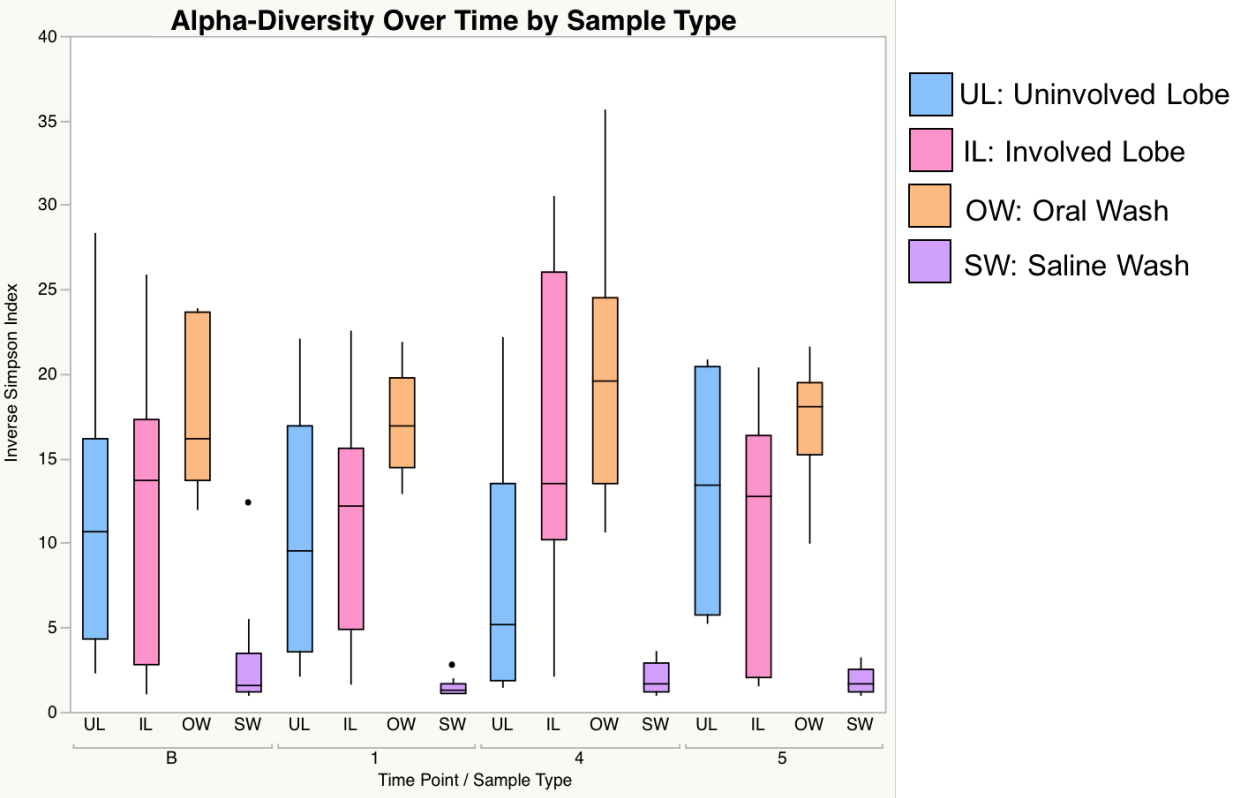

Figure 10. Lung microbiome diversity over the course of *Mtb* infection.

Alpha-diversity of involved lobes (pink) were calculated for each time point. The same was performed with uninvolved lobes (blue), oral washes (orange) and saline bronchoscope control washes (purple).

Overall, these data show that the community structures of the oral cavity and the lung are distinct, confirming that the lung cavity is not just a contamination by the oral flora.

4.3 LUNG MICROBIOTA ARE VARIABLE THROUGHOUT INFECTION

Next, our goal was to determine how the composition of the lung microbiome changes throughout the course of *Mtb* infection. The relative abundance of the top 10 OTUs in BAL samples of involved lobes was determined for each time point for each individual monkey over time (Fig. 11).

Our data show that the relative abundances of the top 10 OTUs over time is variable. It is also apparent that the relative abundances and overall composition of the top 10 OTUs stays relatively stable over time. For example, monkey #15313 displays similar relative abundances of the top 10 OTUs throughout baseline and infection. In contrast, some monkeys display a high amount of variability in the relative abundances and composition of the top 10 OTUs over time. Monkey #16914 displays a wide range of changes in the relative abundances of the OTUs over time. For example, at baseline a high relative abundance of *Moraxellaceae* is seen, but as infection progresses, the relative abundance of this OTU decreases as *Burkholderia* becomes a dominating OTU by month 5. Overall, some macaques display high microbiota variability and some display low amounts of microbiota variability.

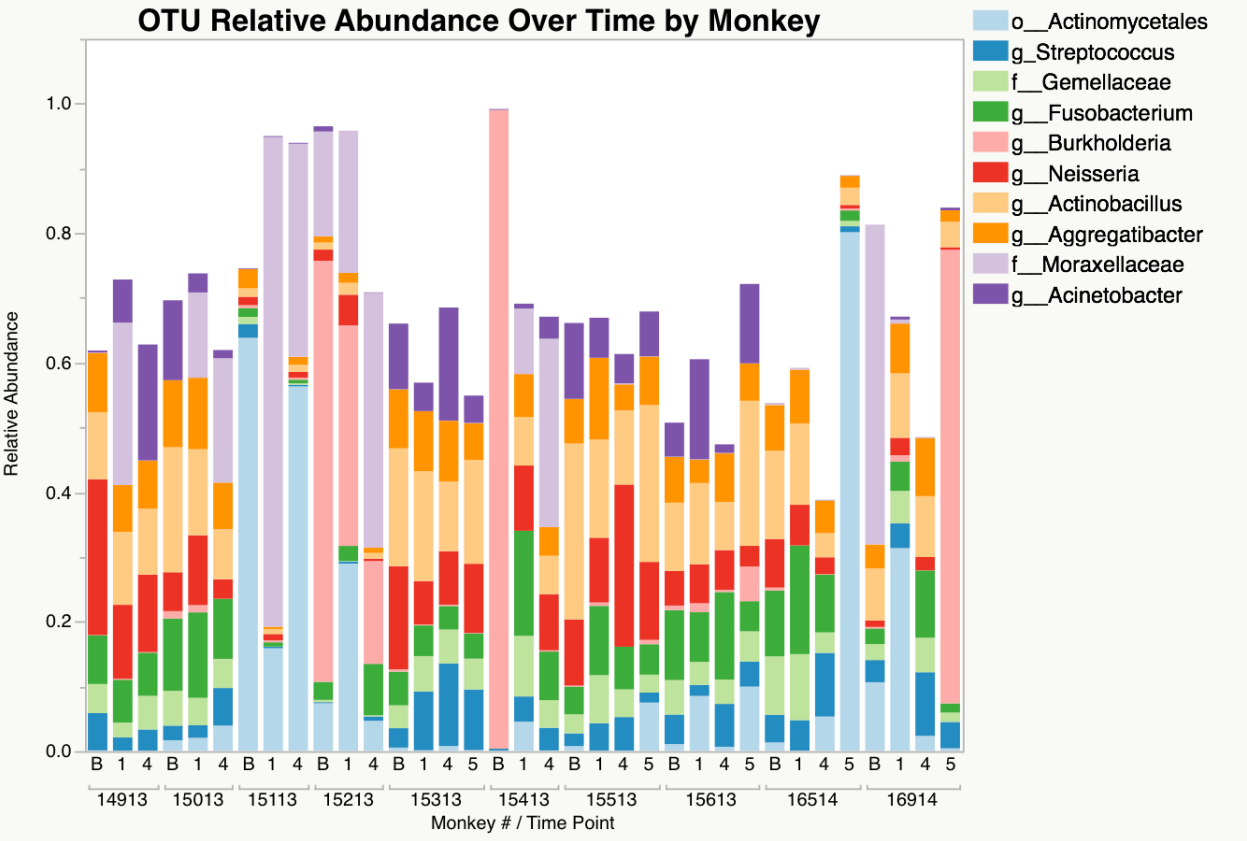

Figure 11. Relative abundance of top 10 generated OTUs over time by macaque in involved lobes

Some monkeys display low amounts of change in the composition of these OTUs over time, while others display high amounts of change. (B = Pre-infection; 1, 4, 5 = 1, 4, 5 months post-infection, respectively). Relative abundance is relative to all OTUs found in the sample.

We investigated how individual OTU relative abundance changes over time between uninvolved and involved lobes. Figure 12 shows uninvolved lobes and involved lobes change differently in terms of relative abundance of OTUs over time. For example, the relative abundance of certain OTUs in the involved lobe, such as *Acinetobacter*, stay relatively stable until 4 months post-infection, followed by a sharp increase. In contrast, the relative abundance of *Acinetobacter* in the uninvolved lobes increase throughout infection, and sharply decline after 4 months post-*Mtb* infection.

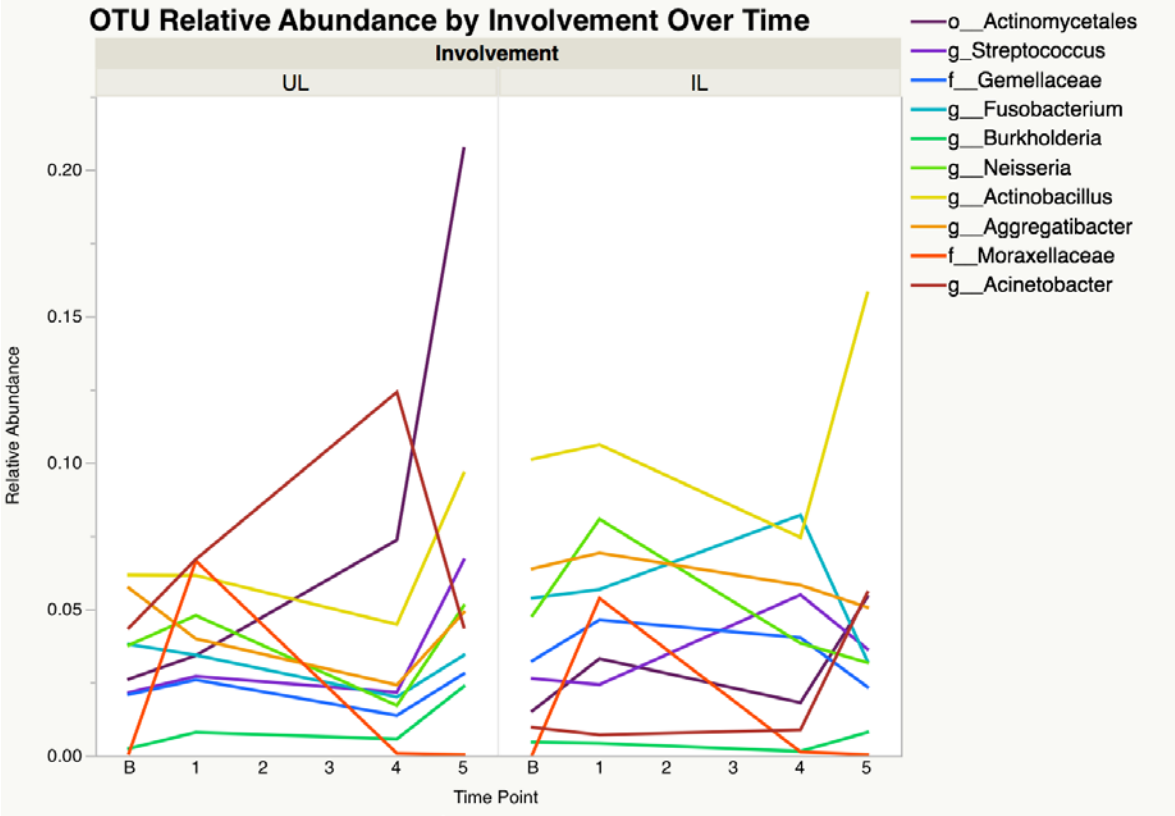

Figure 12. Median OTU relative abundance by involvement over time

We wanted to investigate if there were any differences of OTU relative abundance between involved and uninvolved lobes before and after *Mtb* infection. Our analyses show that before infection, there are no significant differences in relative abundance of the top ten OTUs between involved and uninvolved lobes (Table 3). However, after infection there are significant differences in relative abundance of between involved and uninvolved lobes for specific OTUs. Our results show that post-*Mtb* infection, *Fusobacterium* and *Aggregatibacter* is significantly more relatively abundant in involved lobes, while *Burkholderia* is significantly more relatively abundant in uninvolved lobes (Table 3, Figure 13). Taken together, these data show relative abundance of specific OTUs change post infection, and certain OTUs are more relatively abundant in either involved or uninvolved lobes post-*Mtb* infection, suggesting that *Mtb* infection changes the lung microbiome.

Table 3. Involved vs uninvolved lobes, OTU relative abundance p-values

OTU	pre-*Mtb* p-value	post-*Mtb* p-value
Actinomycetales	0.5208	0.2333
Streptococcus	0.7345	0.8522
Gemellaceae	0.8506	0.0697
Fusobacterium	0.7345	0.0396
Burkholderia	0.2703	0.0481
Neisseria	1	0.2412
Actinobacillus	0.7345	0.2659
Aggregatibacter	0.5208	0.0437
Moraxellaceae	0.8506	0.9765
Acinetobacter	0.7345	0.1208

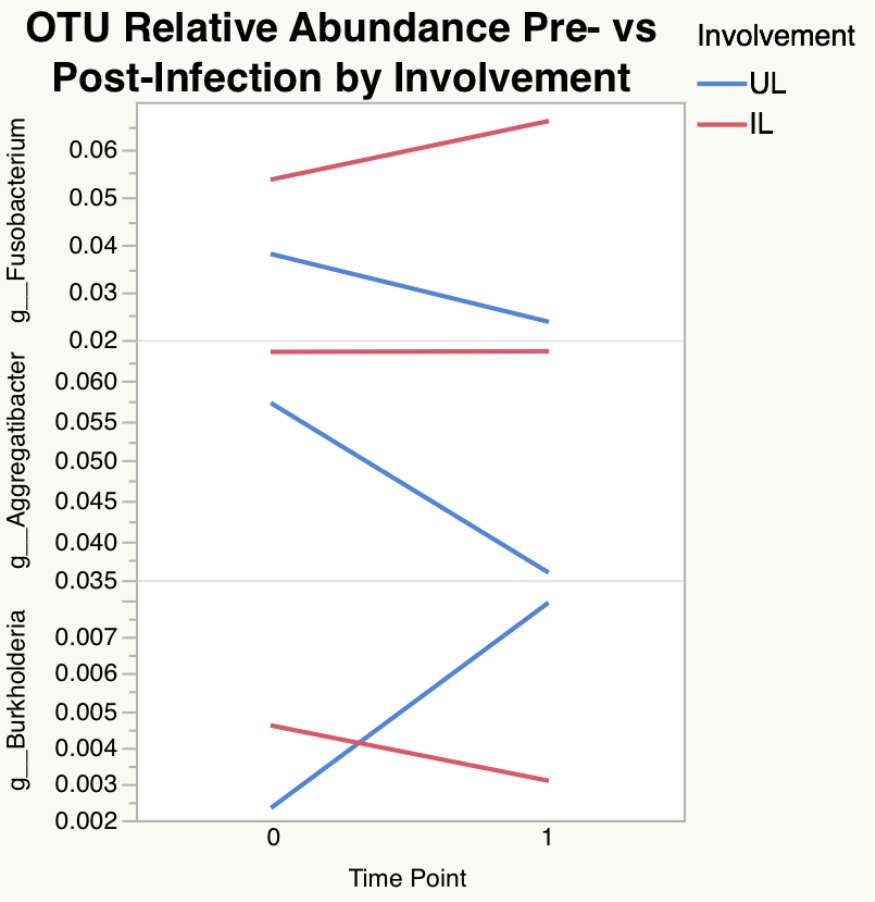

Figure 13. OTU relative abundance pre- vs. post-*Mtb* infection of involved and uninvolved lobes

Median relative abundance is plotted for pre-infection (0) and post-infection (1).

To further investigate at what time point these post-infection differences between involved and uninvolved lobes were the greatest, how OTU relative abundance changes over time was assessed for each time point (Fig. 14). Our analyses show that there is the greatest difference between OTU relative abundance at four months. At four months, involved lobes had significantly higher relative abundances of *Fusobacterium* (p=0.0473) and *Aggregatibacter* (p=0.0387). In contrast, uninvolved lobes had a significantly higher relative abundance of *Burkholderia* (p=0.0201). It is important to note that visually, it looks like there is a higher difference in the uninvolved vs. involved lobes at 5 months post-infection for *Burkholderia* than

at 4 months post-infection. However, there was a lack of 5 month samples (due to treatment or necropsy), reducing the sample size at this time point and ultimately making statistics on this time point difficult. The addition of the second cohort of macaques will improve our sample size, allowing us to fully analyze the differences between uninvolved and involved lobes.

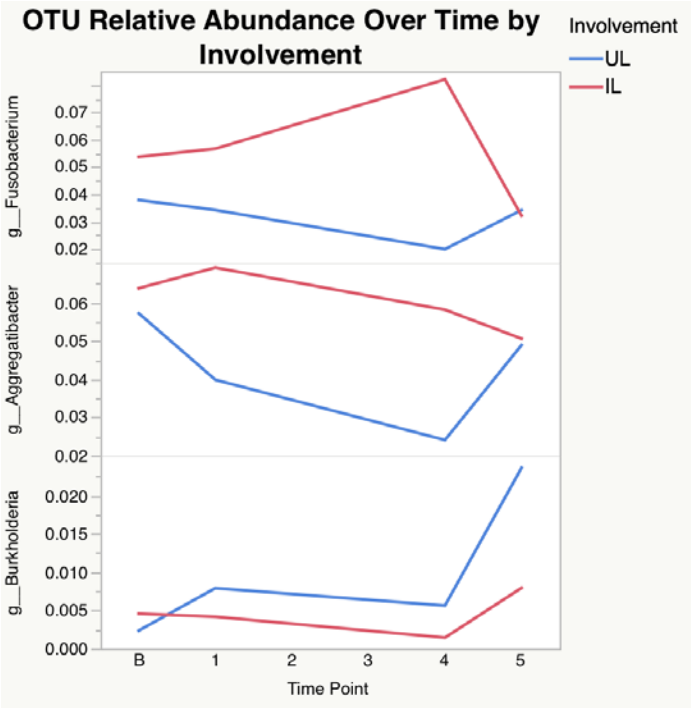

Figure 14. OTU relative abundance (median) over time by involvement

An even deeper investigation of these OTUs show that the relative abundance of OTUs are not only variable over time, but it is also variable among monkeys. Figure 15 shows examples of relative abundances of OTUs over time by individual monkey. The amount of relative abundance per OTU changes throughout time and changes differently in each macaque, showing relative abundance is variable within macaques and among macaques.

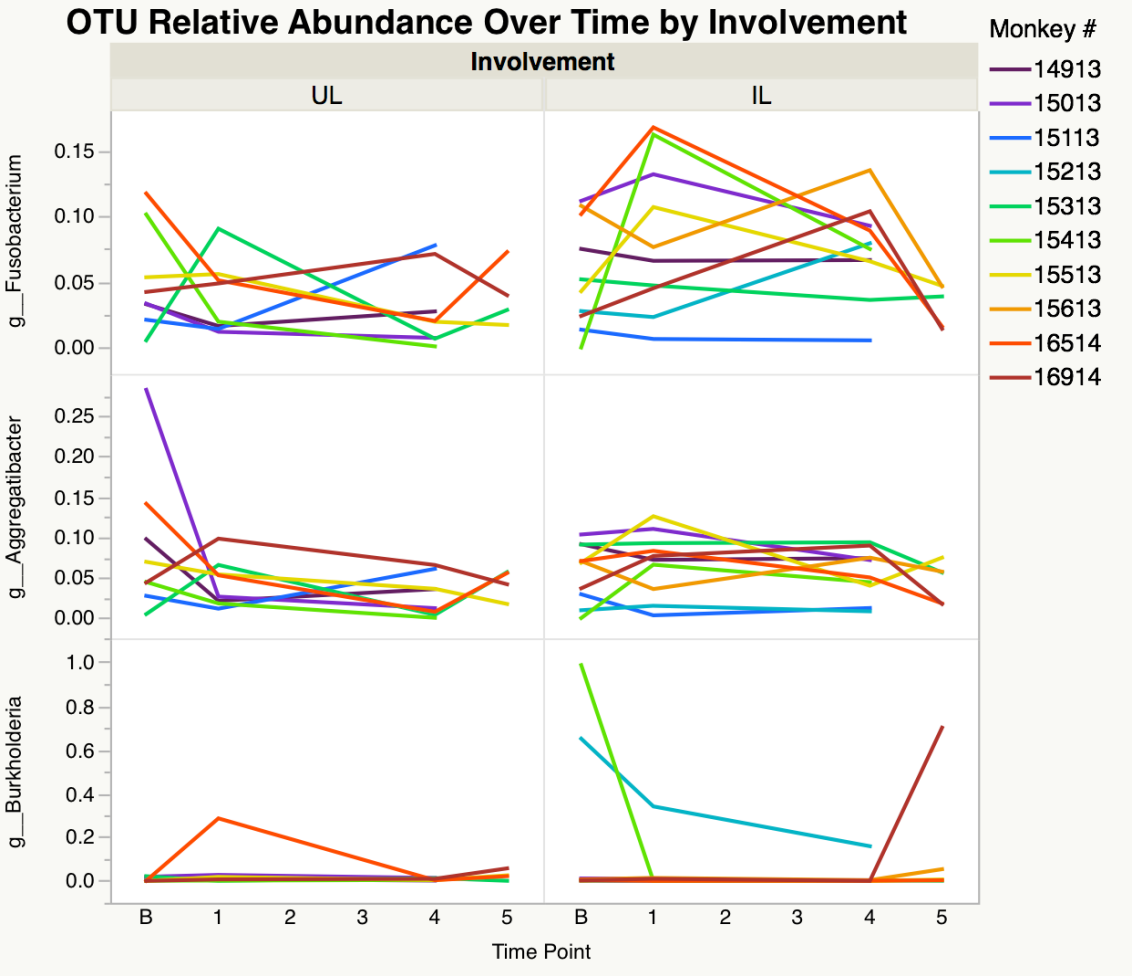

Figure 15. Relative abundance of OTUs (median) over time by individual macaque in involved and uninvolved lobes

Next, we assessed how alpha-diversity changes over time. A trend (p= 0.0574) of an increased alpha-diversity existed in involved lung lobes at 4 months post-infection (Fig. 16), confirming that alpha-diversity between involved and uninvolved lobes is variable.

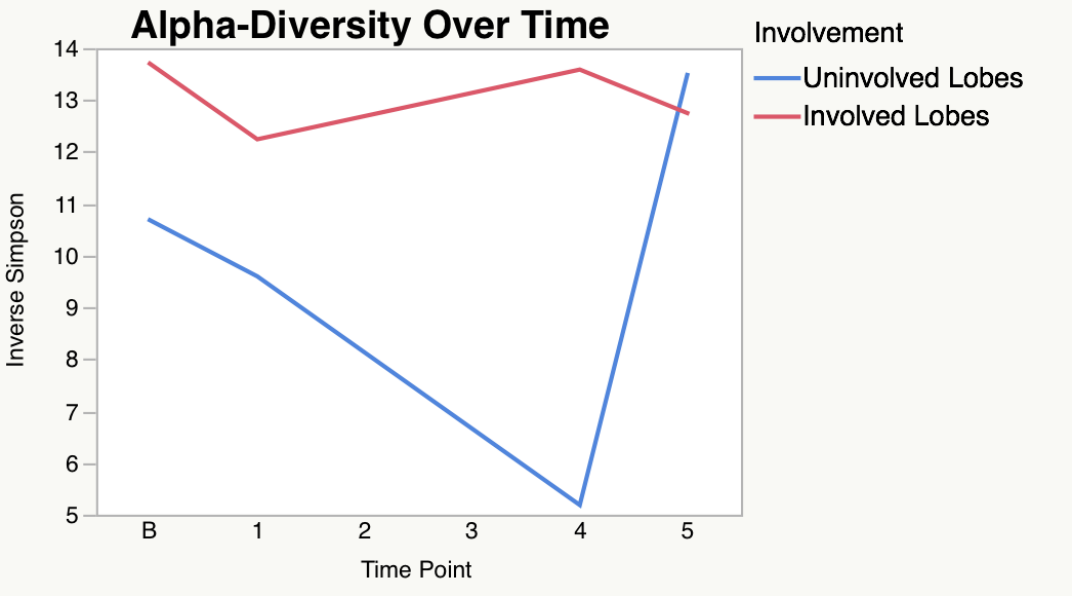

Figure 16. Alpha-diversity (median) over time by involvement

We also evaluated how alpha-diversity changes over time in individual monkeys in involved lobes (Fig. 17). Our data show, that much like relative abundance, diversity is also variable within monkeys and among monkeys throughout time.

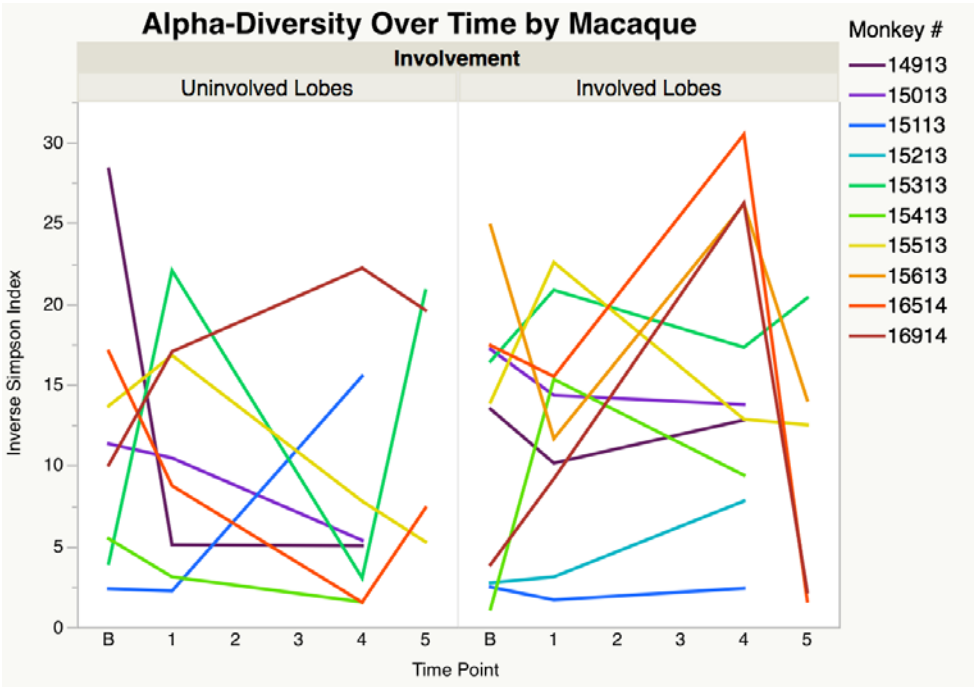

Figure 17. Alpha-diversity (median) over time of uninvolved and involved lung lobes

Spearman **ρ** correlation analyses were performed to test whether there was any correlation between the relative abundances of the top 10 OTUs. We found there were both positive and negative correlations (Fig. 18A-C) with specific OTUs at 4 months post-infection in involved lobes. *Gemellaceae* was significantly positively correlated with *Aggregatibacter* and *Actinobacillus*, showing that when *Gemellaceae* is highly abundant, *Aggregatibacter* and *Actinobacillus* are likely to be highly abundant as well (Fig. 18A-B). In contrast, *Neisseria* was significantly negatively correlated with *Actinomycetales*, showing that when *Neisseria* is highly abundant, *Actinomycetales* is found in lower levels of relative abundance (Fig. 18C).

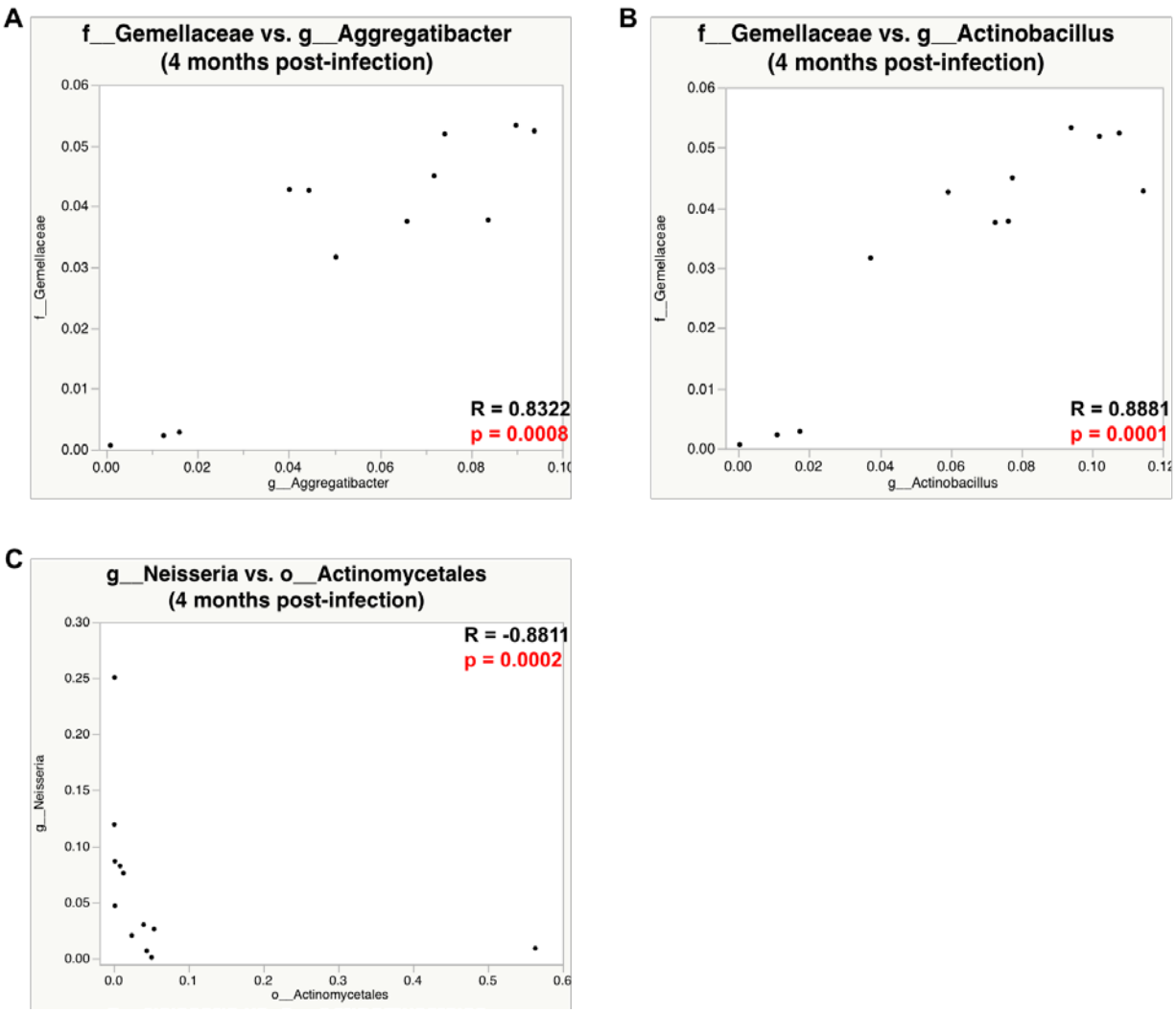

Figure 18. Spearman **ρ** correlations between individual OTUs for all lobes

A) *Gemellaceae* vs. *Aggregatibacter*; B) *Gemellaceae* vs. *Actinobacillus*; C) *Neisseria* vs. *Actinomycetales* show significant ($p \leq 0.05$) correlations.

Taken together, these data show that the change of the lung microbiota is variable throughout time in regards to both OTU relative abundance and alpha-diversity. This variability is seen within individual macaques over time and among different macaques. Certain bacterial OTUs are characteristic of either involved lobes or uninvolved lobes. Lastly, individual OTUs are correlated with each other at 4 months post-*Mtb* infection.

4.4 INFLAMMATION IS VARIABLE THROUGHOUT INFECTION

To assess the variability of inflammation throughout the course of *Mtb* infection, total PET HOT was determined by quantifying FDG avidity, a nonspecific marker of inflammation (Fig. 19). The FDG probe labels metabolically active cells, inferring inflammation is occurring during *Mtb* infection. Our data shows us that total PET HOT changes throughout the course of infection within individual monkeys. An individual macaque at 1 month post-infection can have a relatively low total PET HOT, but by month 4 their total PET HOT may increase to a higher level. By month five, most macaques' total PET HOT levels seems to start to decline. This implies that the amount of inflammation throughout the course of *Mtb* is variable within individual monkeys. Inflammation is also variable between monkeys. Some monkeys maintain a relatively high amount of inflammation (ex. #16814), while other monkeys maintain a relatively low amount of inflammation (ex. 16514) over time.

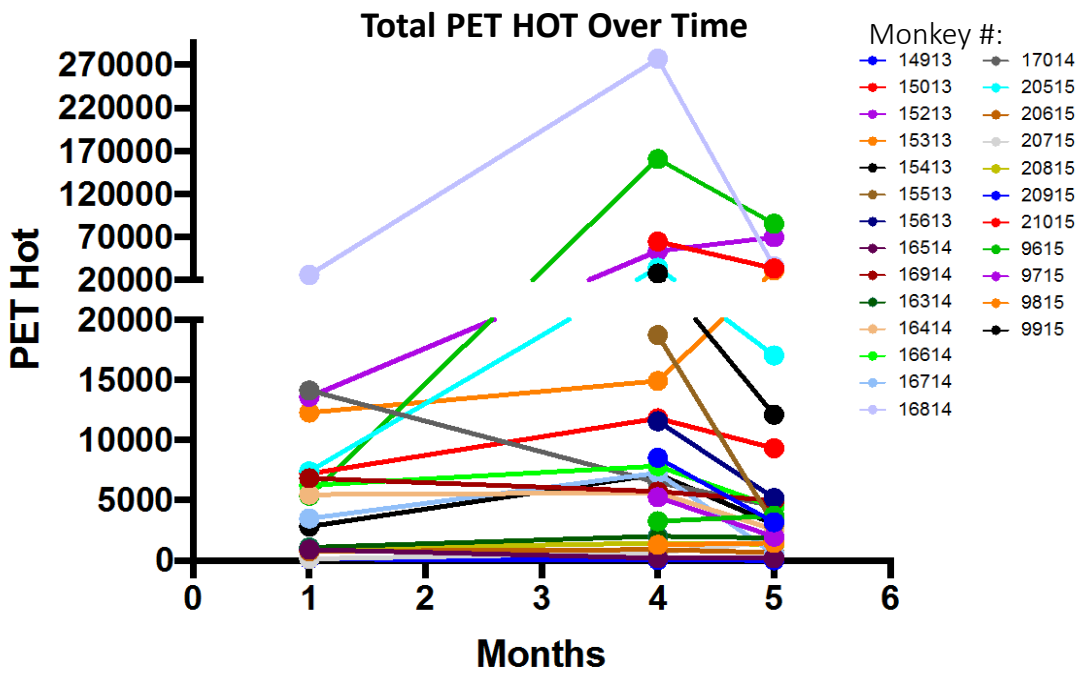

Figure 19. Total PET HOT over the course of *Mtb* infection for N=26 macaques

Each line on the graph represents a different macaque. The amount of inflammation changes throughout infection in individual macaques and is variable between macaques.

We have shown that relative abundance, alpha-diversity, and total PET HOT are variable within and among macaques over the course of infection. To determine whether the variability of total PET HOT over the course of *Mtb* infection correlates with the variability of the microbiota over time, we investigated total PET HOT in regards to both relative abundance of specific OTUs and alpha diversity. Sample size for these analyses were limited to the first cohort of macaques. The following data is preliminary.

A Spearman's **ρ** correlation analysis was performed on the ranges of total PET HOT and ranges of relative abundance of the top ten OTUs. Using the range gave us the overall degree of change. No significant correlations were observed (Table 4), implying that high changes in relative abundance are not correlated with changes in total PET HOT at this time.

Table 4. Spearman's **ρ** correlation values and associated p-values in involved lobes

Variable 1	vs. Variable 2	Spearman's ρ (p-value)
Range (PET HOT)	Range (Actinomycetales)	0.7162
Range (PET HOT)	Range (Streptococcus)	0.6033
Range (PET HOT)	Range (Gemellaceae)	0.3273
Range (PET HOT)	Range (Fusobacterium)	0.9038
Range (PET HOT)	Range (Burkholderia)	0.6111
Range (PET HOT)	Range (Neisseria)	0.9562
Range (PET HOT)	Range (Actinobacillus)	0.7245
Range (PET HOT)	Range (Aggregatibacter)	0.8174
Range (PET HOT)	Range (Moraxellaceae)	0.5051
Range (PET HOT)	Range (Acinetobacter)	0.2082

We then investigated the relationship between alpha-diversity and total PET HOT, allowing us to see whether there were any correlations between the richness and evenness of the lung microbiome and inflammation. A Spearman's **ρ** correlation between total PET HOT and Inverse Simpson Index of involved lobes revealed that alpha-diversity is not associated with inflammation in involved lobes (p=0.4858) within the first cohort of macaques. Our results also show that at this time, changes in total PET HOT are not associated with changes in alpha-diversity over time (p=0.9436).

Lastly, we wanted to know whether a high range in alpha diversity over time could be a predictor of lobe involvement (Fig. 20). Our data show that there is no significant difference between the ranges of diversity between uninvolved and involved lobes (p=0.5404) at this time.

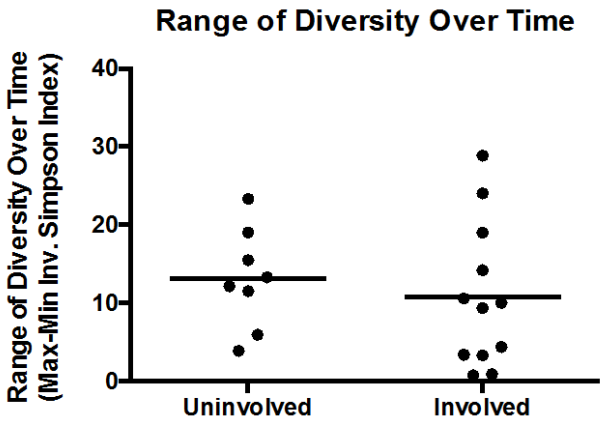

Figure 20. Range of diversity over time in uninvolved and involved lung lobes

A significant difference between uninvolved and involved lobes does not exist ($p = 0.5404$, unpaired t-test).

Taken together, our preliminary results suggest that although PET HOT is variable throughout infection, it is not associated with relative abundance of our top ten OTUs or alpha-diversity. At this time, the range of diversity cannot be used to predict lung inflammation involvement. However, this sample size is very limited, and results may improve when the second cohort of macaques are added to the dataset.

5.0 DISCUSSION

We assessed how the lung microbiome of macaques change throughout the course of *Mtb* infection, and how the composition of the lung microbiome differs from that of the oral cavity. There is a compositional difference between oral wash samples and BAL samples in regards to overall genetic diversity and OTU relative abundance. There is a trend of increased average alpha-diversity within involved lobe sides compared to uninvolved lobes at 4 months post-*Mtb* infection. The overall relative abundances for the 'top ten' OTUs are highly variable throughout infection in some monkeys but stay relatively stable in other monkeys. OTU relative abundance and alpha-diversity of involved lobes is variable over the course of *Mtb* infection within macaques and among macaques. It is also shown that certain bacterial taxa are correlated with each other - *Gemellaceae* was significantly positively correlated with *Aggregatibacter* and *Actinobacillus*. We also investigated how inflammation changes over time due to *Mtb* infection in macaques. Our data show that inflammation over time is variable within individual monkeys and also among macaques. Lastly, we investigated how the changes in the microbiota are associated with inflammation. Our results show that at this time, there is no correlation between PET HOT and relative abundance or alpha-diversity. However, this may change once the second cohort of monkeys is added to the dataset.

5.1 POSSIBLE MECHANISM

Inflammation variability throughout infection and among different macaques is perhaps caused by the vast heterogeneity of *Mtb* infection in general. Disease is not the same within each macaque, and each macaque does not progress throughout infection the same way. Differences in immune responses, granuloma dynamism and heterogeneity, and other factors may play a role in inflammation variability.

The changes of the microbiota abundance and diversity throughout infection may be related to infection, but this remains unclear. Even if microbiota variability is not directly related to inflammation, disease parameters such as CFU, disease spread, and gross pathology score may still be correlated to these changes in the microbiome of the lung. Newly introduced species into the lung post-infection may be a result from increased microaspiration or an increase in other immigration factors, causing an influx of members to travel from the oropharynx down intro the lower airway. Correlations between OTUs may be a result of changes in growth conditions in the lung, or due to microbial interactions between species.

It is interesting to note that multiple ‘peak’ events were observed at 4 months post-*Mtb* infection: peak total PET HOT and largest difference of OTU relative abundance and alpha-diversity between involved and uninvolved lobes. This time point also correlates with the peak of *Mtb* infection. A more thorough investigation of events happening during this time point will be performed. Unfortunately, many questions regarding microbiota variability throughout the course of *Mtb* infection remain unanswered. We suspect that further investigation and analyses will allow us to answer these questions.

5.2 ISSUES

Lung microbiome studies present a number of obstacles regarding sample contamination and bacterial yield. We believe we minimized contamination to the best of our ability (see Methods), and samples were qPCR amplified before sequencing to get a better picture of the relative abundance found in the macaque BAL. Because of high variability in *in vivo* studies, each macaque was assessed individually when seeing how the relative abundance of the 'top ten' OTUs changed over time. The use of the cynomolgus macaque was an ideal model for both *Mtb* infection and lung microbiome assessment. These NHPs present the full spectrum of disease and allowed us to longitudinally sample BAL throughout infection.

Using an NHP model allows us to control many possible confounding variables. However, we do not have control over any antibiotic usage or treatments given to the macaques before they become enrolled in our studies. If macaques were treated with antibiotics before enrollment, this may alter the baseline lung microbiome. When the macaques are brought into the university, quarantine procedures involve standard protocol antibiotic treatments. For example, macaques may get treated for potential parasitic worms (with ivermectin). Nonetheless, we try to limit antibiotic usage, and record any treatments given to the macaques prior to enrollment, allowing us to take note of this when looking at the microbiota pre-*Mtb* infection.

Looking at our data, it is important to note that sample size remains an issue for this cohort. For this first cohort, there are few total PET HOT data for early (1 month) time points. In contrast, the diversity/abundance data is mainly at early time points. Not all macaques were sampled to 5 months post-infection due to treatment or necropsy, and not all PET/CT scans were obtained at 1 month post-*Mtb* infection, leaving many gaps within the datasets (Fig. 21). This

greatly reduced our ideal sample size when assessing correlations between total PET HOT and relative abundance or alpha-diversity over time.

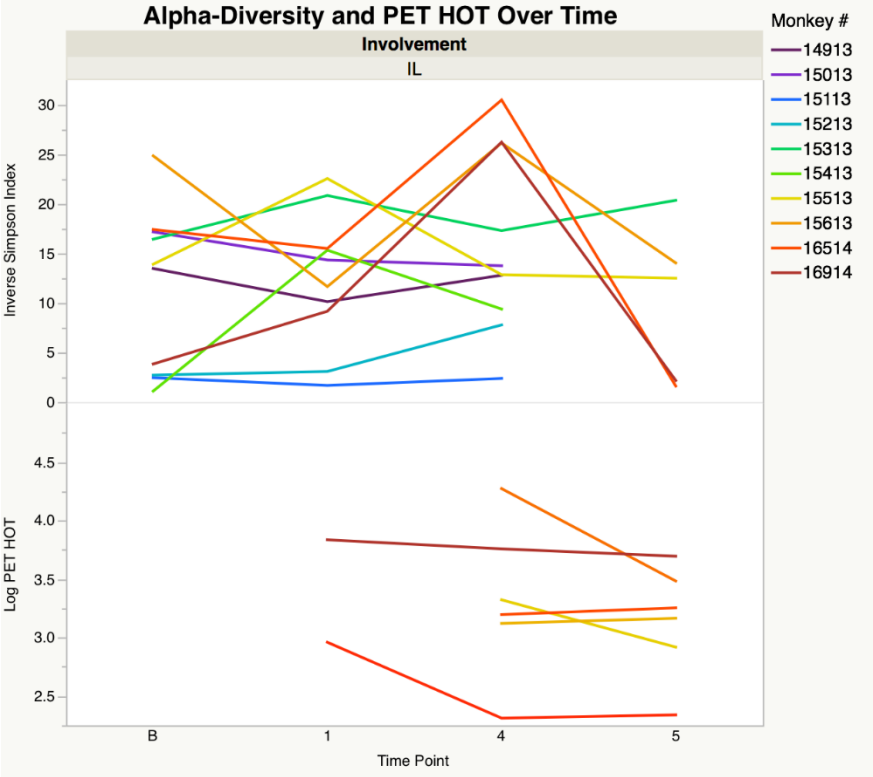

Figure 21. Alpha-diversity and total PET HOT over time by individual macaque

However, the second cohort of macaques contains a fuller data set, improving our data overlap and sample size. This will allow us to fully assess if there is a correlation between inflammation and the changes in the lung microbiome over time.

5.3 FUTURE DIRECTIONS

In the future, we will investigate what may account for some macaques to display a high amount of variability of the relative abundance of the ‘top ten’ OTUs throughout infection and other

macaques stay relatively stable throughout time. All correlation analyses will be rerun once the second cohort of macaques are added to the data, allowing us to improve our sample size.

It is important to note that we did not find *Mtb* in our BAL samples. This may be for a number of reasons: *Mtb* likely clusters together in an OTU (*Actinomycetales*), it is possible that a different region of the 16S rRNA is used to distinguish *Mtb* from other species, or other taxa have outcompeted *Mtb* resulting in a very low relative abundance. We will evaluate this predicament further upon deeper analysis.

Because of the novelty of this type of study, we only assessed early time points of infection (until 5 months post-*Mtb* infection). This is because after this time point, macaques are usually treated or necropsied. This makes it difficult to assess the full spectrum of changes of the microbiome that can occur throughout infection. However, future studies will investigate the effects of both treatment and/or SIV infection on the lung microbiome. We also will be assessing the microbiome and metatranscriptome of individual granulomas.

5.4 PUBLIC HEALTH SIGNIFICANCE AND FINAL THOUGHTS

Overall, the changes in inflammation, microbiome relative, and abundance and diversity throughout the course of *Mtb* infection are variable. This variability is seen throughout time within individual monkeys and also seen among different monkeys. Our data has shown that there is no association between total PET hot and relative abundance of certain OTUs or alpha-diversity. However, with the addition of the second cohort of monkeys and increase of sample size, trends may emerge that could not have been assessed before. These results are important to the field of TB and public health importance because it may have implications for overall lung

health or disease outcome. If associations are found between inflammation and the lung microbiome, alterations to the lung microbiota could serve as a form of treatment to reduce inflammation or decrease the chance of developing active disease.

BIBLIOGRAPHY

1. World Health Organization (WHO) | Global tuberculosis report 2016. *WHO* Available at: http://www.who.int/tb/publications/global_report/en/. (Accessed: 8th March 2017)

2. Pai, M. *et al.* Tuberculosis. *Nat. Rev. Dis. Primer* **2,** 16076 (2016).

3. Zumla, A., Raviglione, M., Hafner, R. & Fordham von Reyn, C. Tuberculosis. *N. Engl. J. Med.* **368,** 745–755 (2013).

4. Brewer, T. F. Preventing Tuberculosis with Bacillus Calmette-Guérin Vaccine: A Meta-Analysis of the Literature. *Clin. Infect. Dis.* **31,** S64–S67 (2000).

5. Daniel, T. M. The history of tuberculosis. *Respir. Med.* **100,** 1862–1870 (2006).

6. O'Garra, A. *et al.* The Immune Response in Tuberculosis. *Annu. Rev. Immunol.* **31,** 475–527 (2013).

7. Gideon, H. P. & Flynn, J. L. Latent tuberculosis: what the host 'sees'? *Immunol. Res.* **50,** 202–212 (2011).

8. Dowdy, D. W., Basu, S. & Andrews, J. R. Is Passive Diagnosis Enough? *Am. J. Respir. Crit. Care Med.* **187,** 543–551 (2013).

9. Kang, B. K. & Schlesinger, L. S. Characterization of Mannose Receptor-Dependent Phagocytosis Mediated by Mycobacterium tuberculosis Lipoarabinomannan. *Infect. Immun.* **66,** 2769 (1998).

10. Esmail, H., Barry, C. E., Young, D. B. & Wilkinson, R. J. The ongoing challenge of latent tuberculosis. *Philos. Trans. R. Soc. B Biol. Sci.* **369,** 20130437–20130437 (2014).

11. Shaler, C. R., Horvath, C., Lai, R. & Xing, Z. Understanding Delayed T-Cell Priming, Lung Recruitment, and Airway Luminal T-Cell Responses in Host Defense against Pulmonary Tuberculosis. *Clin. Dev. Immunol.* **2012,** 1–13 (2012).

12. Sasindran, S. J. & Torrelles, J. B. Mycobacterium Tuberculosis Infection and Inflammation: what is Beneficial for the Host and for the Bacterium? *Front. Microbiol.* **2,** (2011).

13. Nakae, S. *et al.* Antigen-Specific T Cell Sensitization Is Impaired in IL-17-Deficient Mice, Causing Suppression of Allergic Cellular and Humoral Responses. *Immunity* **17,** 375–387 (2002).

14. Ghilardi, N. *et al.* Compromised Humoral and Delayed-Type Hypersensitivity Responses in IL-23-Deficient Mice. *J. Immunol.* **172,** 2827–2833 (2004).

15. Cooper, A. M. Cell mediated immune responses in Tuberculosis. *Annu. Rev. Immunol.* **27,** 393–422 (2009).

16. Shaw, T. C., Thomas, L. H. & Friedland, J. S. Regulation Of IL-10 Secretion After Phagocytosis Of Mycobacterium tuberculosis By Human Monocytic Cells. *Cytokine* **12,** 483–486 (2000).

17. Green, A. M. *et al.* CD4 Regulatory T cells in a Cynomolgus Macaque Model of Mycobacterium tuberculosis Infection. *J. Infect. Dis.* **202,** 533–541 (2010).

18. Almeida, A. S. *et al.* Tuberculosis Is Associated with a Down-Modulatory Lung Immune Response That Impairs Th1-Type Immunity. *J. Immunol.* **183,** 718–731 (2009).

19. Lázár-Molnár, E. *et al.* Programmed death-1 (PD-1)–deficient mice are extraordinarily sensitive to tuberculosis. *Proc. Natl. Acad. Sci. U. S. A.* **107,** 13402–13407 (2010).

20. Ndlovu, H. & Marakalala, M. J. Granulomas and Inflammation: Host-Directed Therapies for Tuberculosis. *Front. Immunol.* **7,** (2016).

21. Korb, V. C., Chuturgoon, A. A. & Moodley, D. Mycobacterium tuberculosis: Manipulator of Protective Immunity. *Int. J. Mol. Sci.* **17,** (2016).

22. Ishimori, T. *et al.* Increased 18F-FDG Uptake in a Model of Inflammation: Concanavalin A-Mediated Lymphocyte Activation. *J. Nucl. Med.* **43,** 658–663 (2002).

23. Lin, P. L. *et al.* Sterilization of granulomas is common in active and latent tuberculosis despite within-host variability in bacterial killing. *Nat. Med.* **20,** 75–79 (2014).

24. Coleman, M. T. *et al.* Early Changes by 18Fluorodeoxyglucose Positron Emission Tomography Coregistered with Computed Tomography Predict Outcome after Mycobacterium tuberculosis Infection in Cynomolgus Macaques. *Infect. Immun.* **82,** 2400–2404 (2014).

25. Lin, P. L. *et al.* Radiologic Responses in Cynomolgus Macaques for Assessing Tuberculosis Chemotherapy Regimens. *Antimicrob. Agents Chemother.* **57,** 4237–4244 (2013).

26. Mattila, J. T. *et al.* Microenvironments in tuberculous granulomas are delineated by distinct populations of macrophage subsets and expression of nitric oxide synthase and arginase isoforms. *J. Immunol. Baltim. Md 1950* **191,** 773–784 (2013).

27. Martin, C. J., Carey, A. F. & Fortune, S. M. A bug's life in the granuloma. *Semin. Immunopathol.* **38,** 213–220 (2016).

28. Cui, L. *et al.* The Microbiome and the Lung. *Ann. Am. Thorac. Soc.* **11,** S227–S232 (2014).

29. Majlessi, L. *et al.* Colonization with Helicobacter is concomitant with modified gut microbiota and drastic failure of the immune control of Mycobacterium tuberculosis. *Mucosal Immunol.* (2017). doi:10.1038/mi.2016.140

30. Khan, N. *et al.* Alteration in the Gut Microbiota Provokes Susceptibility to Tuberculosis. *Front. Immunol.* **7,** (2016).

31. Winglee, K. *et al.* Aerosol Mycobacterium tuberculosis Infection Causes Rapid Loss of Diversity in Gut Microbiota. *PLOS ONE* **9,** e97048 (2014).

32. Hilty, M. *et al.* Disordered Microbial Communities in Asthmatic Airways. *PLoS ONE* **5,** (2010).

33. Dickson, R. P., Erb-Downward, J. R. & Huffnagle, G. B. The Role of the Bacterial Microbiome in Lung Disease. *Expert Rev. Respir. Med.* **7,** 245–257 (2013).

34. Peterson, J. *et al.* The NIH Human Microbiome Project. *Genome Res.* **19,** 2317–2323 (2009).

35. Rogers, G. B. *et al.* Bacterial Diversity in Cases of Lung Infection in Cystic Fibrosis Patients: 16S Ribosomal DNA (rDNA) Length Heterogeneity PCR and 16S rDNA Terminal Restriction Fragment Length Polymorphism Profiling. *J. Clin. Microbiol.* **41,** 3548–3558 (2003).

36. Rogers, G. B. *et al.* Characterization of Bacterial Community Diversity in Cystic Fibrosis Lung Infections by Use of 16S Ribosomal DNA Terminal Restriction Fragment Length Polymorphism Profiling. *J. Clin. Microbiol.* **42,** 5176–5183 (2004).

37. Charlson, E. S. *et al.* Assessing Bacterial Populations in the Lung by Replicate Analysis of Samples from the Upper and Lower Respiratory Tracts. *PLOS ONE* **7,** e42786 (2012).

38. Huffnagle, G. B., Dickson, R. P. & Lukacs, N. W. The respiratory tract microbiome and lung inflammation: a two-way street. *Mucosal Immunol.* **10,** 299–306 (2017).

39. Hubbell, S. P. Neutral theory in community ecology and the hypothesis of functional equivalence. *Funct. Ecol.* **19,** 166–172 (2005).

40. Morris, A. *et al.* Comparison of the Respiratory Microbiome in Healthy Nonsmokers and Smokers. *Am. J. Respir. Crit. Care Med.* **187,** 1067–1075 (2013).

41. Dickson, R. P., Erb-Downward, J. R. & Huffnagle, G. B. Towards an Ecology of the Lung: New Conceptual Models of Pulmonary Microbiology and Pneumonia Pathogenesis. *Lancet Respir. Med.* **2,** 238–246 (2014).

42. Dickson, R. P., Martinez, F. J. & Huffnagle, G. B. The Role of the Microbiome in Exacerbations of Chronic Lung Diseases. *Lancet* **384,** 691–702 (2014).

43. Adami, A. J. & Cervantes, J. L. The Microbiome at the Pulmonary Alveolar Niche: How It Affects the Human Innate Response against Mycobacterium tuberculosis. *Tuberc. Edinb. Scotl.* **95,** 651–658 (2015).

44. Goddard, A. F. *et al.* Direct sampling of cystic fibrosis lungs indicates that DNA-based analyses of upper-airway specimens can misrepresent lung microbiota. *Proc. Natl. Acad. Sci. U. S. A.* **109,** 13769–13774 (2012).

45. Salter, S. J. *et al.* Reagent and laboratory contamination can critically impact sequence-based microbiome analyses. *BMC Biol.* **12,** (2014).

46. Huang, Y. J. *et al.* Airway Microbiota and Bronchial Hyperresponsiveness in Patients with Sub-optimally Controlled Asthma. *J. Allergy Clin. Immunol.* **127,** 372–381.e3 (2011).

47. Erb-Downward, J. R. *et al.* Analysis of the Lung Microbiome in the 'Healthy' Smoker and in COPD. *PLOS ONE* **6,** e16384 (2011).

48. Garcia-Nuñez, M. *et al.* Severity-Related Changes of Bronchial Microbiome in Chronic Obstructive Pulmonary Disease. *J. Clin. Microbiol.* **52,** 4217–4223 (2014).

49. Cox, M. J. *et al.* Airway Microbiota and Pathogen Abundance in Age-Stratified Cystic Fibrosis Patients. *PLOS ONE* **5,** e11044 (2010).

50. Raghu, G. *et al.* High prevalence of abnormal acid gastro-oesophageal reflux in idiopathic pulmonary fibrosis. *Eur. Respir. J.* **27,** 136–142 (2006).

51. Worlitzsch, D. *et al.* Effects of reduced mucus oxygen concentration in airway Pseudomonas infections of cystic fibrosis patients. *J. Clin. Invest.* **109,** 317–325 (2002).

52. Schmidt, A. *et al.* Neutrophil elastase-mediated increase in airway temperature during inflammation. *J. Cyst. Fibros.* **13,** 623–631 (2014).

53. Flierl, M. A. *et al.* Phagocyte-derived catecholamines enhance acute inflammatory injury. *Nature* **449,** 721–725 (2007).

54. Marks, L. R., Davidson, B. A., Knight, P. R. & Hakansson, A. P. Interkingdom Signaling Induces Streptococcus pneumoniae Biofilm Dispersion and Transition from Asymptomatic Colonization to Disease. *mBio* **4,** (2013).

55. Cheung, M. K. *et al.* Sputum Microbiota in Tuberculosis as Revealed by 16S rRNA Pyrosequencing. *PLOS ONE* **8,** e54574 (2013).

56. Botero, L. E. *et al.* Respiratory tract clinical sample selection for microbiota analysis in patients with pulmonary tuberculosis. *Microbiome* **2,** 29 (2014).

57. Wu, J. *et al.* Sputum Microbiota Associated with New, Recurrent and Treatment Failure Tuberculosis. *PLOS ONE* **8,** e83445 (2013).

58. Krishna, P., Jain, A. & Bisen, P. S. Microbiome diversity in the sputum of patients with pulmonary tuberculosis. *Eur. J. Clin. Microbiol. Infect. Dis.* **35,** 1205–1210 (2016).

59. Zhou, Y. *et al.* Correlation between Either Cupriavidus or Porphyromonas and Primary Pulmonary Tuberculosis Found by Analysing the Microbiota in Patients' Bronchoalveolar Lavage Fluid. *PLoS ONE* **10,** (2015).

60. Flynn, J. L., Gideon, H. P., Mattila, J. T. & Lin, P. L. Immunology studies in non-human primate models of tuberculosis. *Immunol. Rev.* **264,** 60–73 (2015).

61. Clifton E Barry, 3rd. The spectrum of latent tuberculosis: rethinking the goals of prophylaxis. *Nat. Rev. Microbiol.* **7,** 845 (2009).

62. Lin, P. L. *et al.* Quantitative Comparison of Active and Latent Tuberculosis in the Cynomolgus Macaque Model. *Infect. Immun.* **77,** 4631–4642 (2009).

63. Lin, P. L. *et al.* Metronidazole prevents reactivation of latent Mycobacterium tuberculosis infection in macaques. *Proc. Natl. Acad. Sci.* **109,** 14188–14193 (2012).

64. Ley, R. E. *et al.* Evolution of Mammals and Their Gut Microbes. *Science* **320,** 1647–1651 (2008).

65. Morris, A. *et al.* Longitudinal analysis of the lung microbiota of cynomolgous macaques during long-term SHIV infection. *Microbiome* **4,** 38 (2016).

66. Lin, P. L. *et al.* Quantitative Comparison of Active and Latent Tuberculosis in the Cynomolgus Macaque Model. *Infect. Immun.* **77,** 4631–4642 (2009).

67. Capuano, S. V. *et al.* Experimental Mycobacterium tuberculosis Infection of Cynomolgus Macaques Closely Resembles the Various Manifestations of Human M. tuberculosis Infection. *Infect. Immun.* **71,** 5831–5844 (2003).